

AUTONOMOUS STAR-IMAGING ATTITUDE SENSOR (ASIAS)

GROUP IX

Matthew N. Cannata 206509640
Michael R. Greene 206973762
Scott J. Mulligan 206841928
Vlad Popovici 206668867

Faculty Advisor: Dr. Brendan Quine
Course Director: Eshrat Arjomandi
Course: ENG 4000

Website: www.asias.ca

Faculty of Science and Engineering
York University

30 April 2007

ABSTRACT

The Autonomous Star-Imaging Attitude Sensor (ASIAS) is a unique star tracker. It has many qualities which very few trackers have fully implemented: small field-of-view, high sample rate, low weight, small dimensions and low cost. The small field-of-view lowers the amount of observed stars and allows for higher positioning accuracy. The high sample rate is achieved through patented star-search algorithms, in an attempt to raise the generally low sample rate of most trackers to the 10Hz of typical satellite subsystems. The low weight and small dimensions are achieved through modern electronics implementation and mission-specific radiation shielding. The low cost can be attributed to all components being of a mass-produced, commercial nature. ASIAS has also been fully developed by a team of four undergraduate engineering students, an engineering professor, an engineering technologist and a machinist on a budget of C\$1000, labour excluded.

ACKNOWLEDGEMENTS

ASIAS would not have been possible without the guidance and software algorithms of Dr. B. Quine, who was the team's advisor; the expertise and efforts of Harvey Emberley, who integrated the electronic components through further designs and extensive testing; and the skill and supervision of Ator Sarkisoff, who spent hours overseeing the construction of the structure and baffle. The team is indebted to these individuals.

TABLE OF CONTENTS

1	INTRODUCTION.....	1
2	PROJECT OBJECTIVES.....	1
3	FIELD OF VIEW ANALYSIS AND SIMULATIONS.....	1
3.1	ASIAS Field of View.....	1
3.2	Computer Simulation for Determining Field of View.....	2
3.3	Simulation Results.....	4
4	OPTICS.....	7
4.1	ASIAS Image Sensor.....	7
4.2	Optical Architecture.....	10
5	ELECTRONICS.....	11
5.1	Electronic Components.....	11
5.2	LabView Interface.....	12
6	SOFTWARE ALGORITHMS.....	13
6.1	Data Analysis.....	13
6.1.1	Centroiding Algorithm.....	14
6.1.2	Image Testing.....	15
6.1.3	Relative Motion of Stars in Sequential Images.....	15
6.1.4	Triad Construction.....	16
6.2	Building the Star Catalogue.....	17
7	HARDWARE DESIGN.....	18
7.1	Functionality Considerations.....	18
7.2	Launch Considerations.....	18
7.3	Space Environment Considerations.....	19
7.4	Baffle Design.....	20
7.5	Electronics Configuration.....	21
7.6	Structure Design.....	22
7.7	Assembly.....	23
7.8	Construction.....	24
8	ACCURACY DETERMINATION OF ASIAS.....	24
9	SPACE QUALIFICATION TESTING.....	26
9.1	Electronic Vibration Test.....	26
9.2	Thermal Vacuum Chamber Test.....	27
10	RESULTS.....	29

11	FINAL BUDGET.....	32
12	HEALTH AND SAFETY.....	33
13	CONCLUSIONS.....	34
14	REFERENCES.....	36
APPENDIX A – Source Code for Algorithms.....		37
A.1	Centroiding Function (centroiding.m)	37
A.2	Data Analysis Algorithm (star_comparison.m)	37
A.3	Average Distance to Center of Image Plane (PixelDist.m)	41
A.4	Field of View Simulation Algorithm (FoV_sim.m)	41
APPENDIX B – Space Qualification Testing.....		44
B.1	Vibration Test Procedure.....	44
B.2	Vibration Test Results.....	45
B.3	Vacuum Test Procedure.....	47
B.4	Vacuum Test Results.....	48
APPENDIX C – Baffle.....		50
APPENDIX D – Microcontroller, Daughter and Optics Board.....		51
APPENDIX E – Structure.....		53
APPENDIX F – LabView Panel and Block Diagram.....		54

LIST OF FIGURES

Figure 3.1 - Histogram for 3.5° field of view.....	5
Figure 3.2 - Histogram for 5° field of view.....	5
Figure 3.3 - Histogram for 6.5° field of view.....	5
Figure 3.4 - Number of stars in reference catalogue.....	7
Figure 4.1 - KAC-9619 ASIAS Image Sensor.....	10
Figure 5.1 - The MC9612CDP512 microcontroller.....	11
Figure 5.2 - Image showing the EVB, daughter board, and optics board.....	12
Figure 6.1 - Pixel intensity mapping.....	15
Figure 6.2 - Centroiding result.....	15
Figure 6.3 - Single triad constructed from ASIAS data.....	16
Figure 6.4 - Star selection diagram.....	17
Figure 7.1 - Typical radiation doses versus shielding in LEO.....	19
Figure 7.2 - Baffle design without threads shown.....	21
Figure 7.3 - Multiple views of the structure, without threads shown.....	23
Figure 7.4 - Exploded view of ASIAS and its components.....	24
Figure 9.1 - ASIAS setup during the vibration test.....	27
Figure 9.2 - ASIAS setup during the vacuum test.....	28
Figure 10.1 - ASIAS image of a simulated star field.....	29
Figure 10.2 - ASIAS image of triad in simulated star field.....	30
Figure 10.3 - ASIAS in its development stage.....	32

1 INTRODUCTION

A star tracker is a sensor that determines spacecraft attitude relative to stars with extremely high accuracy. By analyzing an image containing stars, the angular distance of the sensor's boresight to a star with a known location can be determined. This is then mapped to the spacecraft's reference frame, providing information on the spacecraft's attitude. By comparing successive images, the angular velocity of the craft can then be deduced. Star trackers offer some advantages over other methods of attitude determination: they can accurately determine the spacecraft's attitude and attitude velocity by using an inertial reference frame (the celestial sphere in the short-term), they have no moving parts, and they do not experience loss-of-accuracy from systematic drift. As such, they are used on many current spacecraft and will undoubtedly become more common in the future as they can accurately determine the attitude of a spacecraft at any point in time. In theory, this eliminates the necessity of needing more than one attitude sensor on board, which can greatly reduce the size and cost of spacecraft systems. The goal of the ASIAS project is to implement existing star tracker technology with newly developed ideas in an attempt to enhance the current designs.

2 PROJECT OBJECTIVES

The primary objective of this project is to design a space qualified autonomous star tracker with the capability of accurately determining its attitude relative to the inertially fixed stars in its field of view (FoV). Other secondary objectives include having a small field-of-view, high sample rate, low weight, small dimensions and low cost.

3 FIELD OF VIEW ANALYSIS AND SIMULATIONS

3.1 ASIAS Field of View

One of the defining characteristics of ASIAS is the FoV of the optical system. This is an important characteristic that needs to be determined because it affects almost all aspects of ASIAS since the optical system is the only method of data collection. A large FoV for the optical system means that a large section of the sky will be viewed in each image while a smaller FoV will result in a smaller section of sky visible in each image. An

analysis was done to find out the best FoV size to fit the needs of ASIAS. There are many factors to consider in the analysis, but the main concern is that enough stars need to be identified in each image in order to determine navigational information. If more stars are present in an image, the probability that the software algorithms will be able to identify star formations and determine the spacecraft attitude is increased.

3.2 Computer Simulation for Determining Field of View

Designing the proper FoV size is a complex process so a computer simulation was created to aid in this procedure. The purpose of the simulation is to determine how big the FoV should be in order to guarantee that enough stars will be present in each image. This is done by re-creating the celestial sphere in a simulation using real star coordinates and randomly selecting a location on that sphere which represents the direction that our ASIAS instrument is pointing. The user defines the FoV size of ASIAS that they wish to simulate and the program performs many iterations to collect statistics about how many stars lie within the FoV of the instrument.

The star coordinates used for this simulation are taken from the Hipparcos catalogue which consists of 118209 stars. Specific data was extracted from the star catalogue and was imported into the FoV simulation program. The imported data includes the star identification numbers, the star coordinates in terms of right ascension and declination, proper motion of stars, error values for coordinates and proper motion, and absolute magnitude of each star. The reason that the star magnitude is necessary is because ASIAS will not be able to identify faint stars. Depending on the integration time for each image (amount of time spent for collecting incident light), the CMOS image sensor that images the stars will only be able to detect stars below a certain visible magnitude.

Once this star magnitude cutoff value is determined, the Hipparcos star catalogue is truncated to leave only stars brighter than the specified cutoff magnitude. Early estimates showed that a star magnitude cutoff value between +7.0 and +8.0 would be implemented. Taking a conservative approach and estimating that ASIAS would only detect stars brighter than +7.0, then the star catalogue was truncated to only 14977 remaining stars.

The remaining stars were projected onto a unit sphere using their right ascension and declination coordinates to simulate a realistic celestial sphere as seen from Earth. ASIAS is assumed to be at the exact center of the unit sphere and able to look at the entire inner surface of the simulated celestial sphere.

The simulation also generates a random position on the unit sphere that represents the pointing direction of ASIAS. In the simulation, the pointing direction of ASIAS is always a random sky location that is found by generating Cartesian coordinates within a unit box. But only the randomly generated locations that lie within the unit sphere are kept, and the locations that lie outside the unit sphere are thrown away. The remaining Cartesian coordinates are converted to right ascension and declination values so they can be projected onto the unit sphere and recreate the celestial sphere. The process of generating random Cartesian coordinates and then converting them to spherical coordinates is needed instead of just generating random spherical coordinates. This process is necessary to achieve truly random sky positions since randomly generated spherical coordinates tend to collect at the poles, which corrupts the purpose of the simulation [3].

Once the true star locations are projected onto a unit sphere and a random sky location is chosen, the angular distance between the random sky location and each star is computed. Any stars that lie within an angular distance equal to half the FoV from the random sky location are assumed to be in the FoV of the instrument.

To compute the angular distance between the random sky location and the stars, it is necessary to compare the vectors that connect the center of the unit sphere to the locations of interest on the surface of the unit sphere. This is done by using the definition of the dot product, shown below

$$a \cdot b = |a||b|\cos(\theta)$$

The formula defining the dot product can be rearranged to yield the angular distance between 2 vectors,

$$\theta = \arccos \left(\frac{\mathbf{a} \cdot \mathbf{b}}{|\mathbf{a}| |\mathbf{b}|} \right)$$

However, since we know that points \mathbf{A} and \mathbf{B} lie on the surface of the unit sphere this means that the magnitude of vectors \mathbf{a} and \mathbf{b} are: $|\mathbf{a}| = 1$ & $|\mathbf{b}| = 1$. This reduces the previous equation to the one presented below which is used to calculate the angular distance between these points on a unit sphere,

$$\theta = \arccos (\mathbf{a} \cdot \mathbf{b})$$

The number of stars within the specified angular distance is counted to yield the total number of stars within the FoV of ASIAS. This approach results in a circular FoV even though the true FoV will be rectangular due to the rectangular image plane. This assumption is practical since the circular FoV underestimates the area within the FoV when compared to an equivalent rectangular FoV. This knowledge ensures that the real life observations will in fact be better than the simulated observations attained from this program, which is a must in any type of simulation.

3.3 Simulation Results

The figures presented below are histograms created by the simulation program. The histograms represent the amount of stars present within the FoV for 10,000 randomly selected sky locations. The three histograms below show statistical data for FoV sizes of 3.5° , 5° , and 6.5° respectively with a constant magnitude cutoff value of +7.

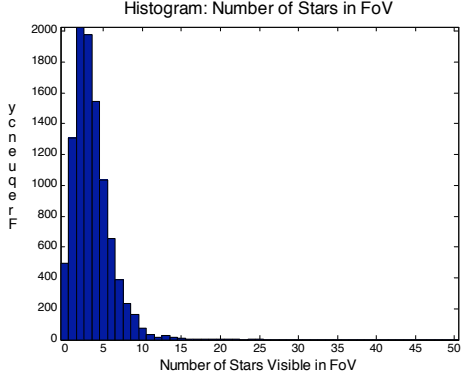


Figure 3.1 - Histogram for 3.5° FoV

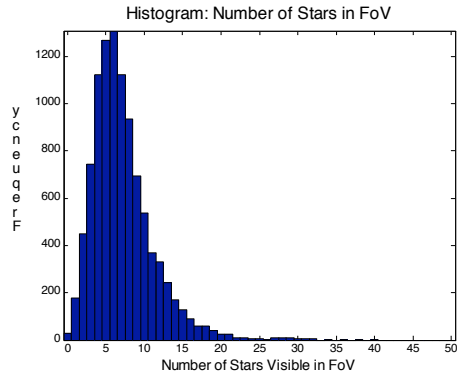


Figure 3.2 - Histogram for 5° FoV

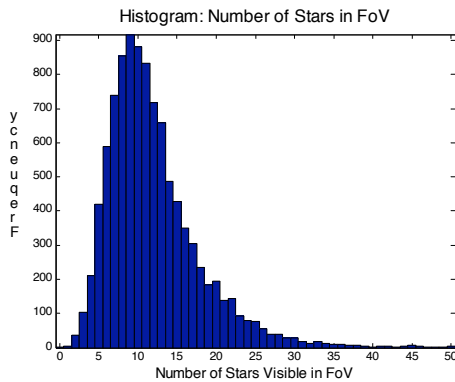


Figure 3.3 - Histogram for 6.5° FoV

The histograms show that the FoV simulation yields the expected results, with more stars visible for large FoVs. The percentage of 10,000 iterations that had five or more stars visible in the FoV was also an important statistic. Five stars were chosen as the threshold because at least three stars are needed to perform the star identification algorithm that determines spacecraft attitude. Identifying five stars in each image allows a margin of error since some stars will not always be found or correctly identified in the onboard star catalogue.

To fully utilize the FoV simulation program, a data table was created to better understand the influence of FoV size and star magnitude cut-off values. The table presented below varies the FoV size and star magnitude cut-off in the simulation program to yield a value that represents the percentage of 10,000 sky locations that have at least five of more stars in the FoV. The error in this approach varies as $1/\sqrt{N}$, where N is the

number of iterations. This corresponds to an error of approximately 1 in every 100 cases. This will provide values that are accurate enough to perform an adequate analysis.

Table 3.1 - Percentage of cases with at least 5 stars in the field of view

Based on 10,000 randomly selected sky locations for each test run (Error of apx. 1/100)

Mag. Cutoff	Field of View (Degrees)											
	2.5	3.0	3.5	4.0	4.5	5.0	5.5	6.0	6.5	7.0	7.5	8.0
5.0	0.0002	0.0002	0.0007	0.0018	0.0040	0.0070	0.0121	0.0181	0.0291	0.0350	0.0520	0.0715
5.5	0.0003	0.0014	0.0038	0.0064	0.0166	0.0307	0.0480	0.0656	0.0972	0.1494	0.1927	0.2489
6.0	0.0023	0.0061	0.0191	0.0336	0.0649	0.1162	0.1798	0.2578	0.3424	0.4348	0.5292	0.6193
6.5	0.0118	0.0305	0.0701	0.1506	0.2478	0.3660	0.4897	0.6254	0.7326	0.8168	0.8896	0.9358
7.0	0.0541	0.1342	0.2704	0.4257	0.6008	0.7419	0.8514	0.9177	0.9668	0.9828	0.9946	0.9980
7.5	0.1946	0.3899	0.6082	0.7860	0.8942	0.9615	0.9854	0.9972	0.9992	0.9998	1	1
8.0	0.4895	0.7512	0.9070	0.9745	0.9948	0.9991	0.9999	1	1	1	1	1
8.5	0.7882	0.9462	0.9922	0.9995	1	1	1	1	1	1	1	1
9.0	0.9563	0.9979	1	1	1	1	1	1	1	1	1	1
9.5	0.9920	0.9999	1	1	1	1	1	1	1	1	1	1
10.0	0.9960	1	1	1	1	1	1	1	1	1	1	1

This table is a powerful analysis tool because it shows numerous FoV sizes and how each size will affect the mission deliverables. One of the requirements that were set for ASIAS is that it should have 98% availability. The ASIAS team defines ‘availability’ for this mission as the ability to form at least one triad from a star image captured by ASIAS. Also, as discussed earlier, it was decided that at least 5 stars must be present in an image to ensure that a triad will be successfully formed and will allow attitude information to be resolved. Any values in the table that are above the 98% availability threshold have been highlighted since they meet the ASIAS specifications. It is now possible to use this analysis to help choose a FoV size for ASIAS that will meet our mission requirements.

One additional factor that was considered when choosing a FoV size was that a smaller star catalogue onboard ASIAS would be optimal compared to a larger star catalogue. This is because a large star catalogue requires more storage room and takes more processing time to search when making star comparisons. The amount of stars in a reference catalogue grows exponentially as the star cut-off magnitude increases, so it would be optimal to use the smallest possible catalogue that still ensures that enough stars will be found.

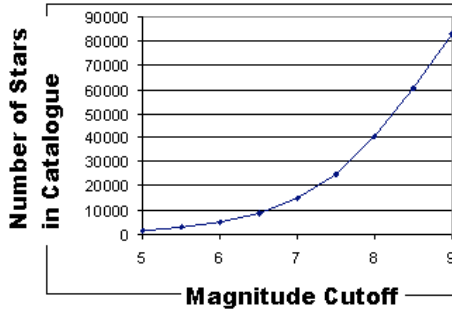


**Figure 3.4 - Number of Stars in Reference Catalogue
(Data taken from the Hipparcos star catalogue)**

After examining the benefits and drawbacks of many different FoV sizes, this simulation has lead to the suggestion that ASIAS should have a FoV size of *5 degrees* with a magnitude cut-off value of approximately *+7.65*. The magnitude cut-off value of *+7.65* will require an onboard star catalogue with roughly 29,406 pre-identified stars. By using the FoV simulation program, we found that this setup for ASIAS will provide an availability of about 98.62%. (IE: At least 5 stars in the FoV for 98.62% of collected images) Using these parameters, there will be an average of *14.07* stars in each image.

4 OPTICS

4.1 ASIAS Image Sensor

The camera sensor is one of the most important components of the ASIAS star tracker since it's responsible for capturing the star images needed for the attitude determination software. The two most popular and available technologies for imaging applications are Charged Couple Devices (CCDs) and Complementary Metal Oxide Semiconductors (CMOSs). Both of these image sensors excel at different applications and the appropriate choice for the star tracker design was based on a careful analysis of many of their characteristics. After extensive research from various papers and internet sources it was decided that this project would use a CMOS chip. This decision was based on the fact that CMOS sensors have the following properties which are particularly advantageous for a space application such as ASIAS [1]:

- 1) CMOS chips are available at much lower costs than CCDs . The cost of the image sensor was very important to ASIAS since the project had a limited budget of \$1000 and it was necessary to acquire an inexpensive but good quality image sensor.
- 2) The power consumption of CMOS sensors is five to ten times than the CCDs. Power consideration is important for ASIAS, since it is an instrument that is integrated on a spacecraft or satellite, where power consumption is very limited. The CMOS technology allows a reduction in power needed to operate the image sensor, therefore making it very desirable for use in space applications. The ASIAS image sensor currently requires a small power of 168 mW.
- 3) CMOS sensors are more radiation resistant than CCDs. The fact that CMOS image sensors can withstand more radiation than CCDs is an incredible advantage in a space application. ASIAS is designed to fly on spacecraft that are susceptible to a lot of radiation from the inner and outer electron belts, solar events, galactic cosmic rays and many other sources and it requires an image sensor capable of withstanding a significant amount of radiation.
- 4) CMOS sensors consist of a higher level of integration on a single chip, thus providing a reduction in size and a potential increase in performance. The fact that the CMOS image sensor is imbedded on a single chip along with most of the electronic components required to run it means that it can be greatly reduced in size. ASIAS is designed to operate on nanosatellite and microsatellite missions and it is imperative that its size is reduced as much as possible.
- 5) CMOS sensors have the unique “windowing” ability which allows reading out a region of interest on an image. The CMOS image sensor “windowing” mode is the last main advantage for using CMOS technology onboard the ASIAS instrument. This mode allows higher speed readout for the region of interest and faster image processing and is therefore ideal for efficient and precision object tracking.

The ASIAS team purchased two KODAK image sensors to use in the final star tracker design. The chosen CMOS image sensor, which can be seen in Figure 4.1 was Kodak's KAC-9619 and its cost was approximately CAD\$30 for each unit. This particular model operates in monochromatic mode and has a resolution of 648 (H) x 488 (V) and a range of up to 30 frames per second. The monochromatic aspect suits ASIAS very well since it reduces the storage memory required and also provides better resolutions. The 648 (H) x 488 (V) resolution of this CMOS image sensor is more than adequate for the attitude analysis determination software and in fact only a windowed portion of the chip is used by ASIAS to increase image acquisition speed and processing time. Table 4.1 depicts the important specifications of the ASIAS image sensor.

Key Specifications

Array Format	Total: 664H x 504V Active: 648H x 488V
Effective Image Area	Total: 4.98mm x 3.78 mm Active: 4.86 mm x 3.66 mm
Optical Format	1/3"
Pixel Size	7.5µm x 7.5µm
Video Outputs	8,10 & 12 Bit Digital
Frame Rate	30 frames per second
Dynamic Range	62dB in linear mode 110dB in non linear mode
Electronic Shutter	Rolling reset
FPN	0.1%
PRNU	1.5%
Sensitivity	5 V/lux.s
Quantum Efficiency	27%
Fill Factor	47%
Package	48 CLCC
Single Supply	3.3 V +/-10%
Power Consumption	168 mW
Operating Temp	-40 to 85°C

Table 4.1 – KAC-9619 ASIAS Image Sensor Specifications

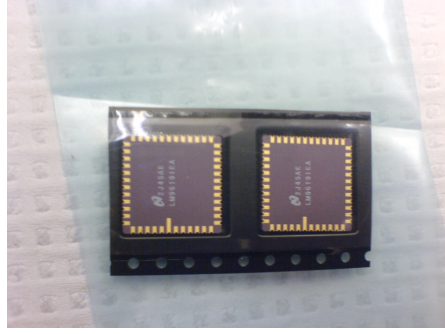


Figure 4.1 – KAC-9619 ASIAS Image Sensor

4.2 Optical Architecture

After running numerous analyses to determine the FoV of ASIAS, 5° was chosen as it was the most reasonable angle that met the mission objectives. Using this angle, the necessary lens focal length f was found to be 55.7mm, by the relation $f = r_d / \tan(\theta_{FOV} / 2)$ [5] where r_d is the radius of the sensor (or more typically, half the width). The optimal quality factor Q for most star cameras is 2 [2], and using $D = 2.44\lambda f Q / d$ [5], where λ is the wavelength of light (lenses optimized for 587.6nm) and d is the size of each pixel on the sensor ($7.5\mu\text{m}$), the aperture of the lens D is calculated to be 21.3mm.

The lens with the closest parameters to the theoretical D and f was found at Edmund Optics. The lens is an achromatic doublet, which reduces picture aberrations, and has a focal length of 50mm and a diameter of 25mm. This lens is coated with magnesium fluoride that acts as an anti-reflection coating, increasing the transmission properties of the lens. Magnesium fluoride has been extensively tested in space as a lens coating and due to its radiation resistance and resistance to atomic oxygen, it is sufficient for a short term Low Earth Orbit (LEO) mission [6].

This makes the revised FoV for ASIAS 5.565° due to constraints in the optical design. Also, the quality factor for this setup will be 2.62. The FoV simulation program was re-run with the new FoV size to determine new characteristics of ASIAS. The simulation was run with a FoV of 5.565° and star cut-off magnitude of +7.4 to yield an average of 13.43 stars per image and 5 or more stars in an image 98.20% of the time. These newly

defined characteristics are important for the section that examines the accuracy of the star tracker.

5 ELECTRONICS

5.1 Electronic Components

The star tracker electronics consists of three circuit boards: the evaluation board (EVB), equipped with the microcontroller running an 8-bit CPU, the optics board built around a CMOS sensor, and a 'daughter' board which relays information from the optics board to the EVB, and is equipped with a voltage regulator. Figure 5.1 show the microcontroller board used in the star tracker.



Figure 5.1 - The MC9612CDP512 microcontroller

This particular microcontroller has an xgate (acts like a dual core processor) with a potential to run at 80 MHz, however this mode it is not currently active. The CPU uses 8 bit data, 16 bit address, and runs at 48 MHz which represents overclocking from the nominal speed of 40 MHz. The EVB has 512k of flash memory, and 32k paged ram. The optics board was designed by Harvey Emberly, an engineering technologist from York University. The Kodak KAC-9619 CMOS sensor is mounted on the optics board, and is set to free running mode at 20 MHz with a 20/31 pixel clock (stepped down). The CMOS has a 688(H)x488(V) resolution, however the sample window has been decreased to 48x86 to increase the overall running speed of the system.

The sensor electronics and microcontroller communicate with IIC communication protocol serial. The microcontroller reads data working under interrupt and loads the data

on the falling edge of the pixel clock. The EVB is interfaced serially through a standard 9-pin RS232 port. The 3.3V power supply and ground are also supplied through this interface. The output is hexadecimal data containing a 2-byte header, a 2-byte error code, a 4-byte origin (2 row, 2 column), 4128 bytes of image data and a 1-byte even parity. For the purpose of the demonstration, a LabView VI has been written to interface with ASIAS. Figure 5.2 shows the EVB, optics board, and ‘daughter board’.

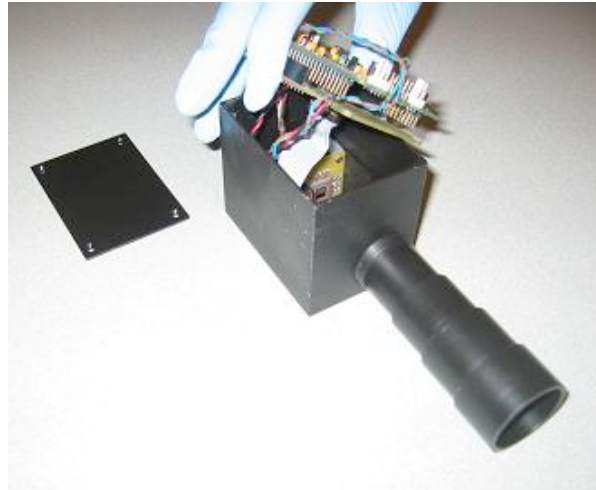


Figure 5.2: Image showing, from top down, the EVB, the daughter board and the optics board

5.2 LabView Interface

The LabView programming environment was used for the image acquisition algorithm, which outputs the image from the raw data obtained from the microcontroller via a serial interface bus. The built-in VISA interface is used to establish communication between LabView and ASIAS. The information is sent serially in a continuous flow of raw data. For this reason, a 2 byte header is inserted at the beginning of each package of data. As the data is coming in, each byte is analyzed and once the header ‘()’ is located, the data acquisition can begin. As mentioned previously, the 6 bytes immediately following the header represent an error code, and the row and column of the origin of the sample window on the CMOS. The following 4128 bytes are hexadecimal data containing the image and the packet ends with a one byte even parity. This data is placed in a 2D array and sent to an intensity graph which outputs the monochromatic image, and prints it to the screen. While the data appears on the screen, it is being written to a binary file which

appears a 48 by 86 array of numbers from 0 to 255. This file is called by the data analysis algorithm, which is written in MATLAB.

6 SOFTWARE ALGORITHMS

One of the most challenging aspects of this project is the computer software algorithms that analyze the data collected by ASIAS. There are two main sections of the software analysis package. The first section is responsible for analyzing data received from the ASIAS camera system so it can identify stars and construct triads for each image. The second section is responsible for constructing the star catalogue that holds pre-calculated triad information for a specific amount of stars. These two sections are ultimately merged together as the information gathered in the first section is compared to the star catalogue in the second section.

All algorithms used for this project were developed in MATLAB and selected algorithms are presented in Appendix A. Throughout the software design process it was important to keep in mind that the algorithms should be as efficient as possible. MATLAB has a built in profile function that helps debug and optimize MATLAB algorithms by tracking their execution time for each line and makes suggestions on how to improve coding. The profile function was a useful analysis tool because it was able to pinpoint where bottlenecks occurred in the algorithms so that they could be fixed.

It is important to note that the software discussed in section 6.1 was created by the ASIAS team, while the software discussed in section 6.2 dealing with the star catalogue was created by Professor B. Quine. The software algorithms were generously offered to the ASIAS team by Quine since the task of creating star comparison catalogues is a difficult undertaking that is beyond the scope of this project.

6.1 Data Analysis

The data analysis package was created in MATLAB and has the capability to identify stars and create multiple star triads from each image captured by ASIAS. The ASIAS camera system is currently set up to directly send information to a LabView visual interface. The camera system sends information about each pixel in the CMOS imaging

chip to LabView. Each pixel has a specific intensity value that is proportional to the amount of photons collected by that pixel in a certain time interval. So each pixel of the CMOS chip is mapped with a corresponding intensity value in the range of 0 to 255 where ‘255’ represents the maximum intensity. Now that each pixel has an intensity value, it is assumed that the high intensity pixels are due to starlight that is incident on the image plane.

One approach may be to claim that all high intensity pixels above a chosen threshold are stars. This approach is valid, however the location of the identified stars can only be found to an accuracy of one pixel since the star location may fall anywhere within the pixel. This is why star trackers employ a method termed ‘centroding’ to find the star locations to sub-pixel accuracy.

6.1.1 *Centroding Algorithm*

Star trackers employ a method termed ‘centroding’ to find star locations to sub-pixel accuracy based on the relative intensity of adjacent pixels. Centroding is an approach that intentionally defocuses the incoming light so that the resultant image is slightly blurred and the incident starlight falls onto an array of pixels instead of just one single pixel. This approach uses a centroding algorithm to compare the intensity of the brightest central pixel with the intensity of neighbouring pixels in order to find the sub-pixel location of the star. The particular algorithm created for ASIAS defocuses the starlight so that it falls upon a 3 by 3 array of pixels. The centroding algorithm [4] shown below outputs centroid offset values (X_C , Y_C) that represent the offset of the calculated star location from the center of the central pixel of the 3 by 3 array.

$$X_C = \frac{\sum_i \sum_j I(i, j) \cdot i}{\sum_i \sum_j I(i, j)} \quad Y_C = \frac{\sum_i \sum_j I(i, j) \cdot j}{\sum_i \sum_j I(i, j)}$$

This algorithm defines a star as a central pixel that has an intensity value higher than a computed threshold and higher than each of its eight adjacent pixels. In addition, any location that has 3 or more adjacent pixels of the maximum intensity value is discarded and not considered a star. This is because the centroding algorithm may be hard to apply to a very bright object resulting in an inaccurate star location.

6.1.2 Image Testing

The centroiding process described above was applied to an image acquired by ASIAS. The data analysis algorithm was used to import a chart of intensity values from LabView that represents the image captured by ASIAS. The 3 by 3 array of pixels displayed in Figure 6.1 is a close up of one identified star.

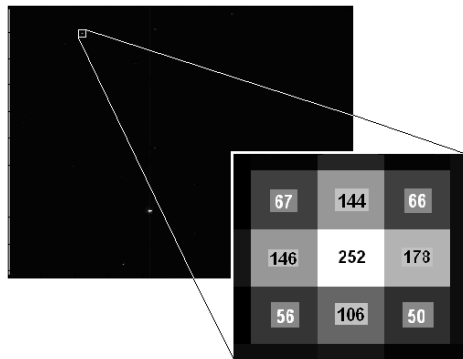


Figure 6.1 – Pixel Intensity Mapping

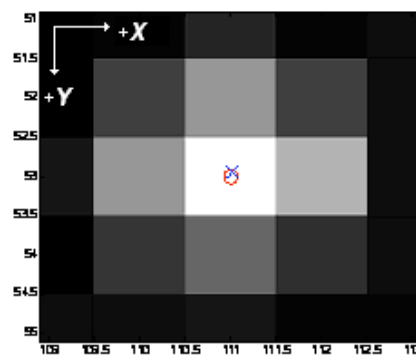


Figure 6.2 – Centroiding Result

The centroiding algorithm was applied to the same 3 by 3 array of pixels and it output centroid offset values of: $X_C = 0.0235$ pixels and $Y_C = -0.0610$ pixels. These values are represented graphically in Figure 6.2 where the red circle shows the centre of the central pixel and the blue 'X' shows the calculated centroid offset which is the sub-pixel location of the star. Notice how the center location of the star is not exactly in the center of the pixel.

6.1.3 Relative Motion of Stars in Sequential Images

ASIAS gathers information about spacecraft angular rate based on the relative motion of stars between successive images. It was necessary to expand the previous algorithms so that they have the capability to compare multiple images. Once a star is successfully identified in subsequent images, the relative angular distance between the star's locations can be found. To do this it is important to account for stars that move out of the FoV, new stars that move into the FoV, and other stars that are not re-acquired when comparing successive images. By knowing the relative motion of stars and their direction of motion in successive images, ASIAS can estimate the angular rate of the spacecraft.

6.1.4 Triad Construction

An algorithm was created to analyze all identified stars to build a star triad or multiple star triads with stars that meet the specified criteria. A triad is made up of a central star and two secondary stars. The triad is only constructed if the secondary stars lie within a certain distance range from the central star to make sure they are not too close or too far away from the central star. Once a triad is constructed, the three angular distances between the stars are calculated. Multiple triads can be constructed for a single image to increase the probability that a triad will be successfully identified when compared to the star catalogue.

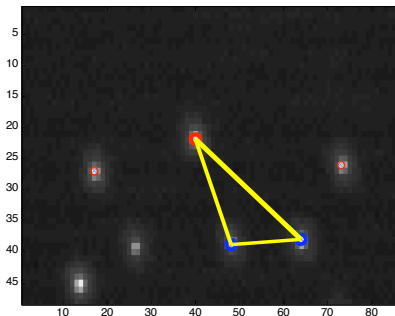


Figure 6.3 – Single Triad Constructed from ASIAS Data

The following is a list of criteria that are used to construct a star triad:

- The central star is identified first as the best choice that is near the center of the image.
- The two secondary stars are chosen as the brightest stars that lie within the allowable area which is between two rings specifying the minimum and maximum angular separation distances.
- The stars that make up the triad are numbered in the following way to be consistent with the star comparison catalogue developed by Quine [3]:

Star 1 – The central star.

Star 2 – The star that forms the anticlockwise edge of the triad rotated about star 1.

Star 3 – The star that forms the clockwise edge of the triad.

- The angular separation distances between the three stars are ordered in the following way to be consistent with the star comparison catalogue [3]:

Star 1 - Star 2 Star 1 – Star 3 Star 2 – Star 3

Specific criteria that were selected to optimize the performance of ASIAS are displayed in Figure 6.4. For the 5.6 degree (0.09774 rad) FoV, the minimum angular separation radius was set to 0.00160 radians, and the maximum angular separation radius was set to 0.0234 radians.

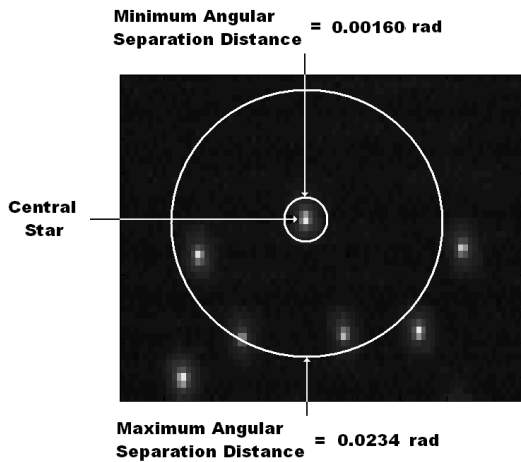


Figure 6.4 – Star Selection Diagram

6.2 Building the Star Catalogue

Once the three angular distance values in a triad are calculated, they are compared to pre-calculated angular distance values stored in a reference catalogue. Since the set of three angular distances in a triad are almost certainly unique, it is possible to identify the three stars that make up the triad.

There are certain scenarios that should be accounted for when comparing triads to the reference catalogue: multiple potential triads or no triads found at all. The algorithm was created so that ASIAS can function properly even if no triads are found. The algorithm will simply skip that image, and readjust the attitude after the next successful triad match. If multiple triads are returned after a catalogue search then the triad chosen is the one that is angularly closest to the stars identified in the previous image.

To build the catalogue, it was necessary to input all the parameters that are specific to ASIAS. Necessary inputs to build the catalogue include: the FoV size, the maximum visible star magnitude, the focal length, the pixel size, pixel offset, the maximum and minimum allowable star separation, image size, the number of triads to construct per image, the number of triads to construct per star, and the number of total triad patterns to create in the catalogue.

7 HARDWARE DESIGN

7.1 Functionality Considerations

A port for power and data transfer is needed in ASIAS's structure, which allows the component to communicate with the satellite. An area in the structure is allocated for this, and space has been included for an upgraded electronic system (required for onboard processing).

The optical system requires a light-tight area, so the structure is designed to not have any areas where light can enter directly (with the exception of the lens port). The inside of the structure is light-absorbing, so that any stray light which has entered through the lens will not reflect towards the CMOS sensor. A baffle is necessary as well, to prevent excess light from entering through the lens, and the lens' position from the sensor is adjustable for focusing.

The thermal environment in ASIAS needs be maintained in order to prevent the electronics from overheating. Passive means of thermal control are used because of their simplicity; space between the electronic components allows for heat radiation, and a light-absorbing structure removes this heat. The overall temperature of ASIAS is to be maintained by the spacecraft bus.

7.2 Launch Considerations

The launch of ASIAS will put much stress on the structure. Loading from the launch vehicle comes in the forms of sine-equivalent, random and shock vibrations, and the structure is designed around these. One of the most common microsatellite launch

vehicles is the Soyuz rocket, which may deliver up to a constant 5G's of force on any axis of it's payload. ASIAS has a sturdy structure so it will remain functional after testing and launch.

7.3 Space Environment Considerations

ASIAS is designed to be a component on a short-duration mission in LEO. A less radiation-hardened design is therefore possible because there will be less total accumulated dose on the internal components. Nevertheless, radiation mitigation is important because a high dose may degrade the functionality of the onboard electronics. Both the mission duration and the height of orbit about Earth are proportional to the amount of radiation received. ASIAS is also designed to be an internal subsystem in a spacecraft bus, which will provide further structural shielding. Typical radiation doses for a satellite in LEO are shown in Figure 7.1 [7].

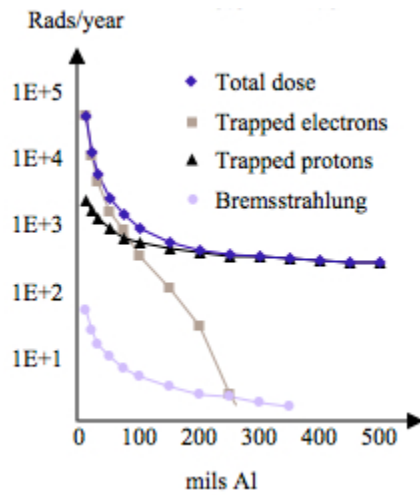


Figure 7.1 – Typical radiation doses versus shielding in LEO

The most common methods of mitigating radiation from the space environment are the use of structural and spot-shields, or radiation-hardened electronics. Radiation-hardened parts are generally more expensive, less available, and not much more effective than commercial parts [8] and as such ASIAS relies solely on shielding to reduce the harmful effects of space radiation. ASIAS is designed to have a minimal amount of shielding because of the diminishing effectiveness-to-mass ratio, and this is provided by the

structure. The amount of shielding is defined by the integrity of the structure.

ASIAS is designed so that the near-vacuum in LEO will not affect the mission's integrity. The enclosing structure will not be air-tight, so that the depressurization during testing or launch will not load the structure or cause much outgassing. This is very important, as the slightest outgassing while in orbit could affect the functionality of the mission by applying unknown forces or material depositions on the spacecraft.

Since ASIAS is assumed to be enclosed in a spacecraft bus, it is not designed for atomic oxygen degradation, which is an issue for LEO satellites [5]. ASIAS's only components that are visible on the satellite's surface are the baffle and the lens, and the lens is coated with magnesium fluoride to reduce its reactivity.

7.4 Baffle Design

The baffle is made of a stepped design, to maximize the total internal reflection of incident light. This design reduces the amount of light that enters through the lens by reflecting it back into space [9]. The baffle is made of 6061 aluminum because it is low in weight, strong and inexpensive, and it is 80mils thick in order to provide the strength necessary for the survival of launch. It is of a cylindrical design.

To simplify the components of ASIAS, the baffle also provides a housing for the lens. The lens is secured between two plastic rings threaded into the baffle. A ridge inside of the baffle provides the lens stop. The baffle also has an external thread around its base, so that it can be screwed into the structure. This baffle-screw design allows for the distance between the lens and the CMOS sensor (fixed at a position in the structure) to be adjusted to the desired focus. The length of the baffle screw is 1.5", providing a larger contact area between threads so that the baffle will not shear them from the structure during launch. Figure 7.2 shows the design of the baffle.

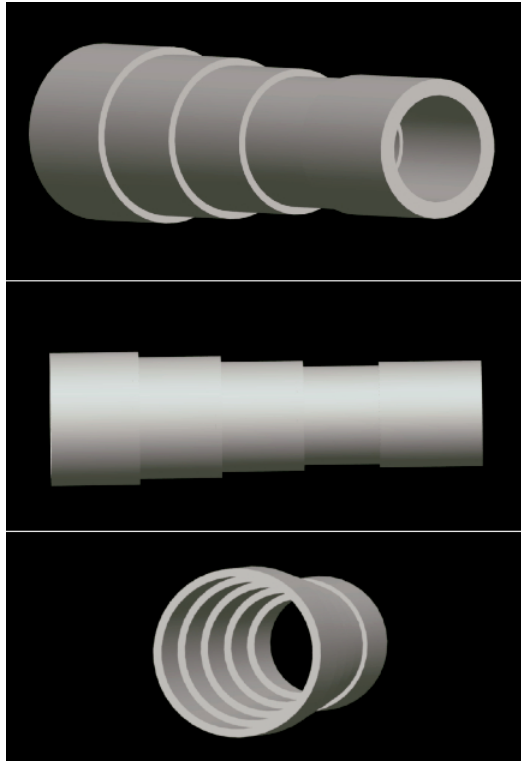


Figure 7.2 – Baffle design without threads shown

The FoV of ASIAS has been designed to be 5.565° , and the baffle possesses a FoV of 6° to not impede on any of the system's optics. This value sets the size of the steps from the lens to 100:7. The length of the baffle determines the sun-rejection angle, and at 4 inches from the lens a 31° rejection angle is provided. This is a typical value of star trackers. The dimensions of the baffle can be found in Appendix C. The baffle is painted a flat black to aid in absorption of light.

7.5 Electronics Configuration

The electronics of ASIAS have been designed to compliment the existing dimensions of the microcontroller. The microcontroller is 2.3x3.25 inches, and the daughter board has been constrained to those dimensions because it is stacked underneath the microcontroller through spacers. The sensor board is underneath the daughter board, stacked perpendicular, and attached to the structure through brackets and a groove. The CMOS sensor is soldered onto the sensor board in alignment with the baffle centerline. There is ample space in between all components so that heat can be radiated to the structure, the electronics can be upgraded, and there is ease of assembly. Figure 7.4 shows the

orientation of these components, and the electronic dimensions can be found in Appendix D.

7.6 Structure Design

ASIAs's structure is made from milled 6061 aluminum. The two parts of the structure are a box to enclose the electronics and its corresponding lid. The box's aluminium walls are 120mils thick on the bottom and on the side of the structure that the threaded hole for the baffle is located, and 80mils elsewhere. This provides the strength necessary for launch survivability and radiation shielding to diminish the total dose on the electronics by two orders of magnitude. The structure has been designed so that the electronics fit tightly in it, providing lateral stability. There is a port in the back of the box for an RS232 9-pin connector to be mounted. The baffle hole is encased by 200 mils of aluminum extending 1.5 inches into the structure, and is threaded on the inside so that the baffle can screw into it.

There are three pillars in the corners not containing the baffle hole, extending 1.4 inches from the bottom of the structure. These are tapped for 4-40 screws, and there is a 4-40 hole in the corresponding baffle corner. The daughter board and microcontroller are secured to these pillars through a stack of spacers. There is a double groove in the bottom of the box so that the sensor board can be secured to the structure, and it is also mounted to the back pillars through brackets. There are 8 4-40 holes tapped into the bottom of the structure as a means of mounting ASIAS to the satellite. Figure 7.3 shows the box.

The lid is 80mils thick and is notched around its edges so that it sits inside of the box. There are 4-40 holes in its corners so that a screw can secure the lid to the electronics spacers and the box.

The box and lid are painted a flat black, so that light and heat absorbed from ASIAS's internal components are radiated into the spacecraft's bus.

Appendix E shows the dimensions for the structure.

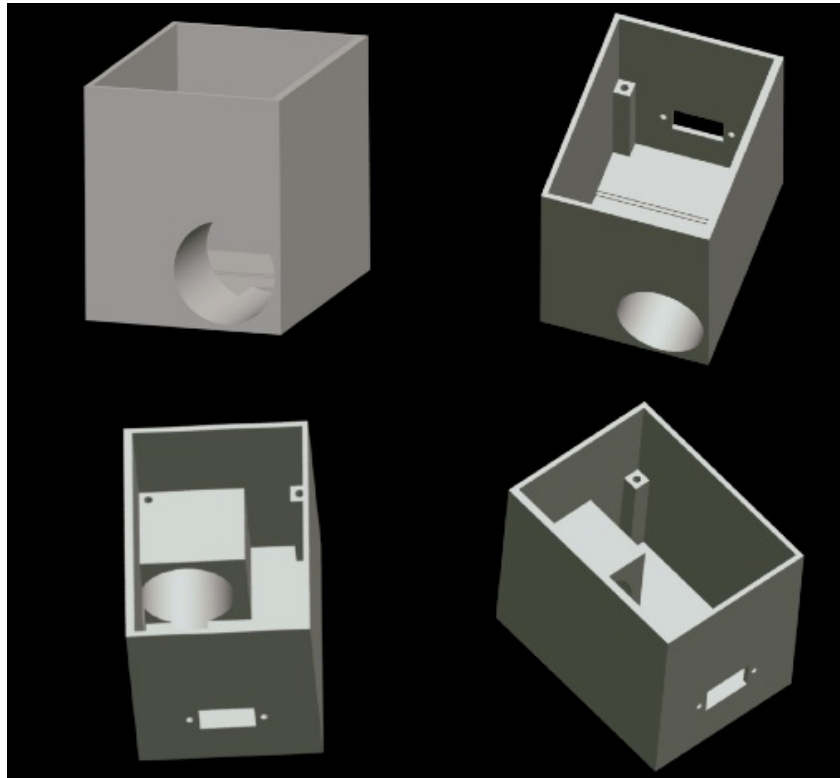


Figure 7.3 – Multiple views of the structure, without threads shown

7.7 Assembly

1. Putting the thin ring at the front of the lens, place the lens down the back of the baffle till it sits on the supporting ridge. Thread the thicker plastic ring behind the lens to secure the lens to the baffle.
2. Mount the brackets onto the sensor board, and then place them on their corresponding pillar supports at the back of the structure. Feed 4-40 threaded rods into the tapped holes in the box.
3. Attach all electronics together. Placing spacers on the rods and in between the daughter board and the microcontroller, slide the daughter board and microcontroller onto the threaded rod. Secure with a threaded spacer acting as a nut on the rod.
4. Place the lid on the box, screwing 4-40 screws into the threaded spacer above the microcontroller.
5. Solder the wires of the electronics onto an RS232 plug, and then screw the plug into the structure.
6. Screw on the baffle, and focus the light by adjusting the amount the baffle is screwed in.

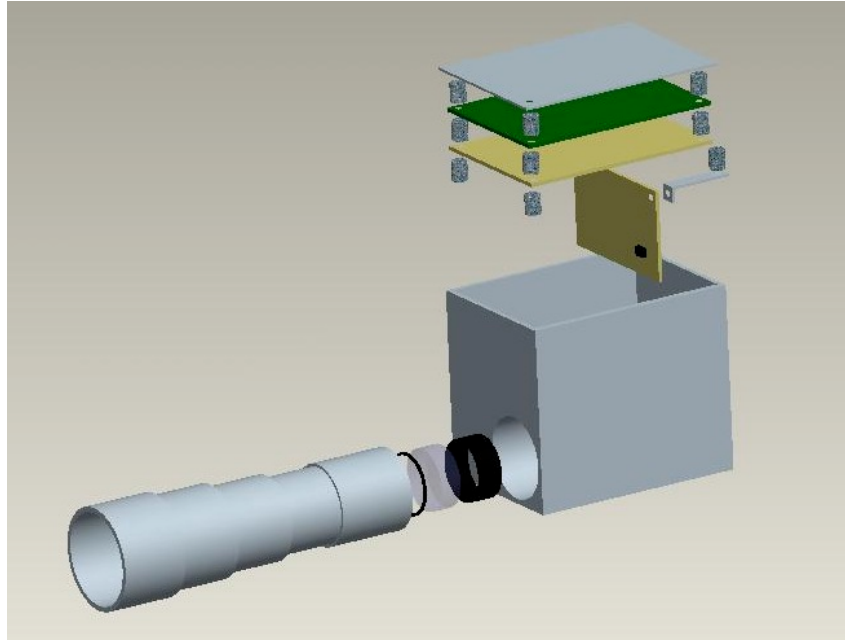


Figure 7.4 – Exploded view of ASIAS and its components

7.8 Construction

The physical construction of the ASIAS instrument took two months and over 100 hours in the student machine shop at York University. The facilities at York University included a lathe and a milling machine which were both crucial in the construction of the star tracker. The cylindrical ASIAS baffle was constructed on the lathe and the ASIAS body was built using the milling machine. Many other tools such as Vernier calipers, sanding paper, drilling bits, rotary cutters, and filing tools were also required during the construction process.

During the construction of ASIAS there were many changes done to the original design in terms of both dimensions and structure layout. This brought forth the engineering process since each construction phase had to be evaluated and verified with the overall design of ASIAS.

8 ACCURACY DETERMINATION OF ASIAS

One of the main goals of a star tracker is to provide reliable and precise 3-axis attitude estimation of a spacecraft. Based on the celestial coordinates of observed stars, it is

possible to calculate the pointing direction of the star tracker and the rotation around that direction. With this information and knowledge of the orientation of the star tracker on the spacecraft, the attitude of the spacecraft can be output in the form of a directional cosine matrix or quaternion.

There are two main ways to increase the accuracy of attitude estimates:

1. Sub-pixel precision of star locations, done by the centroiding algorithm.
2. All stars present in an image contribute to attitude estimation. The increase in accuracy in this case is due to statistical properties of using many stars [2].

Both of these methods are implemented so that ASIAS can produce high accuracy attitude estimates. This is important because it helps determine if ASIAS would be able to meet the needs of current microsatellite and nanosatellite missions, so that it may be considered as a primary instrument for future missions. The accuracy of attitude estimation for ASIAS is predicted by the following calculations that are based upon the FoV simulation discussed earlier, the characteristics of the CMOS image sensor used in ASIAS, and centroiding accuracy measurements.

The Noise Equivalent Angle (NEA)¹ for the cross-boresight (pitch and yaw axes) is approximated by the formula below [2] where FoV is the field of view, $\epsilon_{centroid}$ is the centroiding accuracy, N_{pixel} is the number of pixels across the image plane, and N_{star} is the average number of stars in an image.

$$E_{pitch-yaw} = \frac{FoV \cdot \epsilon_{centroid}}{N_{pixel} \cdot \sqrt{N_{star}}}$$

$$E_{pitch-yaw} = \frac{5.6 \text{ deg} \cdot 0.1}{488 \cdot \sqrt{14.07}} = 1.1014 \text{ arcsec}$$

¹ **Noise Equivalent Angle** is the star tracker's ability to reproduce the same attitude estimates, based on the same observations.

The Noise Equivalent Angle (NEA) for the roll axis is approximated by the following process. The first step is to determine the average distance from a star location on the focal plane to the center of the focal plane. A Monte Carlo simulation was created to find the average distance to the center of the focal plane based on our CMOS image sensor that has dimensions of 648 x 488 pixels. The Monte Carlo simulation randomly generated 1 billion points on the focal plane and approximated that the average distance to the center was $D_{AVG} = 218.6225$ pixels. The average distance (D_{AVG}) can then be used to find the average accuracy about the roll axis [2] based on a single image taken by ASIAS.

$$E_{roll} = \arctan\left(\frac{\varepsilon_{centroid}}{D_{avg}}\right) \cdot \frac{1}{\sqrt{N_{star}}}$$

$$E_{roll} = \arctan\left(\frac{0.1}{218.6225}\right) \cdot \frac{1}{\sqrt{14.07}} = 25.1526 \text{ arcsec}$$

As this analysis shows, the accuracy along the roll axis is far less than the accuracy along the pitch and yaw axes for a star tracker. This is typical for all star trackers which are approximately 5-25 times less accurate in the roll axis. The reason for this discrepancy is that the dimension of the focal length is far greater than the dimensions of the focal plane [2]. None the less, a theoretical average accuracy along the roll axis of 25.1526 arc seconds (6.99×10^{-3} degrees) makes ASIAS comparable to even the most sophisticated star trackers currently available.

9 SPACE QUALIFICATION TESTING

9.1 Electronic Vibration Test

One of the main objectives of this project was to create a space qualified instrument. ASIAS was subjected to two important space qualification tests that were available in the CRESS Lab at York University.

The first test that was run for the ASIAS instrument was a vibration test. The setup for this particular test can be seen in Figure 9.1.



Figure 9.1 – ASIAS setup during the Vibration Test

The vibration test is necessary to see how the ASIAS hardware, structure, and functionality react to launch loads. This was a non-operational test, and ASIAS was turned OFF throughout the entire test run. The test simulated a launch aboard a standard Soyuz system by generating sinusoidal and random waves with amplitudes of up to 5 times the force of gravity (5g load). ASIAS was subjected to these vibrations on both its longitudinal and vertical axes to make sure that it can survive any position configuration aboard a launch vehicle. ASIAS passed the vibration test without any difficulty and the results of the test as well as a more detailed test procedure can be found in Appendix B.

9.2 Thermal Vacuum Chamber Test

The second test that was run for ASIAS was the vacuum test. The setup for this particular test can be seen in Figure 9.2.

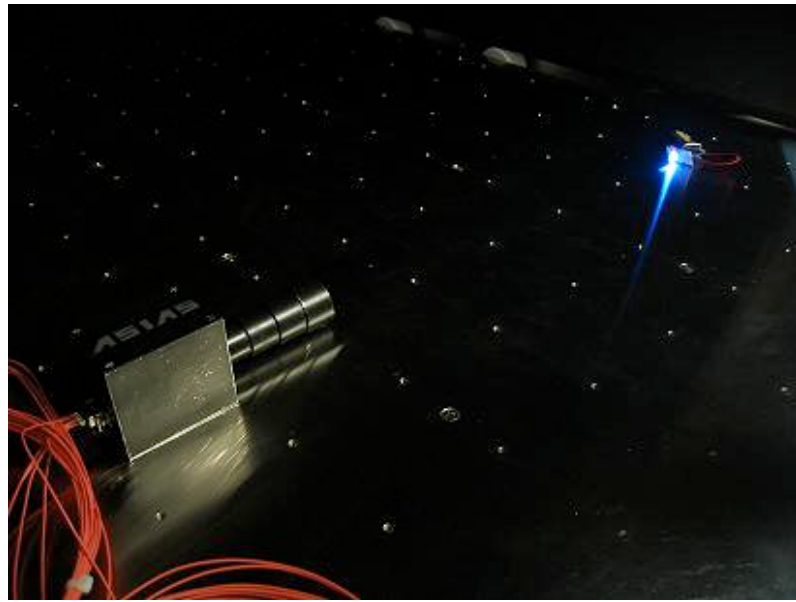


Figure 9.2 – ASIAS setup during the Vacuum Test

The vacuum test is done to see if the instrument is capable of operating in a vacuum environment. Contrary to the vibration test, ASIAS was turned ON throughout the entire test run. ASIAS was pointed at a set of LEDs inside the vacuum chamber to be able to detect any changes in the image quality or image acquisition times as the pressure decreased. The pressure inside the chamber was brought to a final value of 10^{-6} torr, to simulate a low Earth orbit (LEO) environment and ASIAS was maintained at that pressure for a total time of 1.5 hours. Throughout this time no changes were recorded in ASIAS's operation and it was decided that the instrument passed this space qualification test. The results of the vacuum test as well as a more detailed test procedure can be found in Appendix B.

Since ASIAS ended up passing both the vibration and vacuum tests, it is sufficiently space qualified. There are several other tests that could be performed on the instrument, but so far ASIAS is definitely on track for surviving a satellite mission in Earth orbit.

10 RESULTS

Once the construction and the electronic interfacing were complete, ASIAS underwent several operational tests to determine its capabilities as a star tracker. The most important test done up to date was using ASIAS to take pictures of a simulated star field. The star field was created using two 100W light bulbs projecting light through perforated aluminum foil. The test was performed successfully and the results can be seen in Figure 10.1.

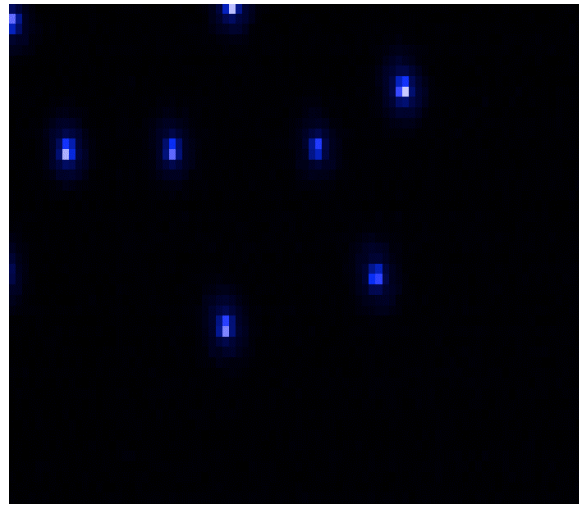


Figure 10.1 – ASIAS image of a simulated star field

At this point in the test, the software component of the project was also tested by running the obtained star image through the triad algorithm. The program was able to successfully detect a triad of stars as shown in Figure 10.2. The star catalogue portion of the software was also used for this part of the test, but no triads were identified since the simulated star field did not represent an accurate representation of star sizes and distances.

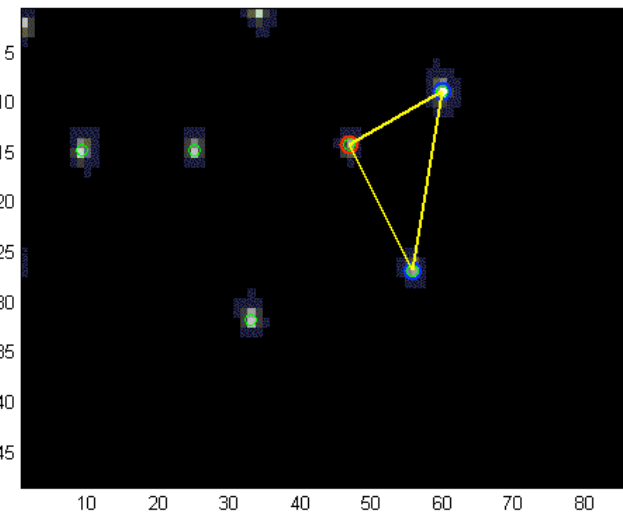


Figure 10.2 – One of the first “triads” detected using an ASIAS image of a simulated star field

This test was deemed very successful and showed that ASIAS could become a working star tracker. Before ASIAS can be classified as a fully working star tracker, it must undergo its most important test which involves a setting with real stars. This test is scheduled to take place between May 1 and May 4, 2007 at the Algonquin Radio Observatory. This location is well-suited for this test since it has minimal noise pollution, thus increasing the amount of stars that could be detected by ASIAS.

Table 10.1 shows several important characteristics and features of ASIAS after it was fully completed and tested.

Mass	555g
Size (without Baffle)	890mm length / 620mm width / 760mm height
Baffle size	100mm length, 420mm to 310mm diameter
Lens	25mm aperture / 50mm focal length
Field of View	0.56° to 5.6°, with 31° baffle sun rejection angle
Microcontroller	MC9612XDP512
Image Sensor	Kodak KAC-9619 monochromatic
Pixel Format	48 x 86 to 480 x 640
Readout Rate	1 HZ max
Power Consumption	1.8W
Pointing Accuracy	25.7 arcseconds, theoretically

Table 10.1 – ASIAS Features and Characteristics

Upon completion of this project, the ASIAS team has agreed that building a camera from scratch, which was done for this project, is not a suitable goal for a fourth year project considering it was not its primary objective. Instead, the suggestion to buy a camera and implement it in the design would have been optimal to ensure that an excessive amount of time was not spent designing a camera, and was instead used to finalize the design of the star tracker as a whole.

ASIAS was fully constructed and assembled on April 10, 2007. Figure 10.3 shows ASIAS in its assembly.

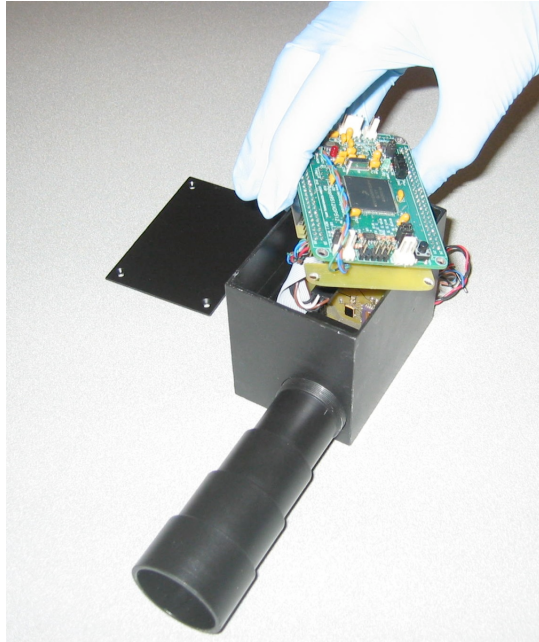


Figure 10.3 – ASIAS in its development stage. Note the regard to cleanliness

At the end of the project, the ASIAS team came up with several improvements to the overall design and construction of the instrument. If the budget was not as restrictive, the structure would have been anodized as opposed to spray-painted. Anodizing has roughly the same optical and thermal properties as paint, and it is highly non-reactive to atomic oxygen. It is also more stable than paint and does not peel as easily when placed under stress. The baffle and structure could have been more accurately milled and lighter if the machine shop had more precise mills and lathes, and smaller cutters, or if a different kind of aluminum was used. 7075 aluminum performs better under fatigue, is stronger and more easily machined than 6061 aluminum [10], but it was not used due to its cost and lack of availability. The baffle could have also been constructed of a different material to decrease its mass. If the budget could support it, a light-sensitive shutter should be used to shield the optical system from over-saturation when the Sun, Earth or the Moon is within the sun-rejection angle.

11 FINAL BUDGET

This project had a planned budget of \$1000 Canadian dollars. Table 11.1 outlines the final ASIAS budget as of April 27, 2007. All of the listed prices are in Canadian dollars

and they include shipping and tax wherever applicable. Any facilities or components of the project that were available at no charge were not included in this budget summary (York's Student Machine shop, microcontroller software development kits, power supplies, etc.)

Project Component	Price
Website Domain Address	\$ 20.00
Website DSN	\$ 10.00
2 x KODAK KAC-9619 Image Sensors	\$ 77.55
2 x 25 mm Optical Lens	\$ 300.00
1 x Aluminum Block (3 in x 4 in x 10 in)	\$ 80.00
1 x Aluminum Cylinder (12 in x 2 in)	\$ 25.00
4 x Printed Circuit Boards (2 x camera + 2 x daughter boards)	\$ 100.00
1 x Rotary Tool Kit	\$ 70.00
Vibration Test @ CRESS Lab	\$ 60.00
Vacuum Test @ CRESS Lab	\$ 60.00
Assortment of Electronic components (resistors, LEDs, 9V batteries, RS232 connectors, electronic screws)	\$ 50.00
Presentation Poster	\$ 75.00
Presentation and Demo-setup supplies	\$ 100.00
TOTAL	\$ 1027.55

Table 11.1 – Final ASIAS Budget as of April 27, 2007

12 HEALTH AND SAFETY

Many phases of this project required a close look at various health and safety aspects in order to ensure the project's success without any injuries or harm to people or the environment.

The first time where health and safety was considered was during the assembly and construction of ASIAS. All of the ASIAS construction required the use of many tools and machinery located in York University's machine shop. A machine shop has potential to cause serious harm and injuries to untrained and inattentive workers. In order to begin building ASIAS, the machine shop required over 10 hours of training on the operation

and health and safety aspects of each machine. This training period was essential in preventing any injuries or harm to the group members in charge of constructing ASIAS.

Another phase of the project that required a good knowledge of health and safety was during the space qualification tests. In order to become a space qualified instrument, ASIAS underwent a vibration test and a vacuum test. Both of these tests had safety procedures that needed to be followed in order to ensure that no harm was done to the environment or the people around. One health aspect of the vibration test was that it generated a substantial amount of noise, and any person confined within the test chamber needed to wear protective sound equipment. The vacuum test required careful monitoring of pressure and temperature and the status of the coarse and cryogenic pumps to make sure that the test was operating at a high level of safety.

By the end of the project, the ASIAS team followed all of the health and safety aspects required for each phase of the project. It was very important to do so in order to ensure that no harm would come to the environment and the people that were involved with ASIAS.

13 CONCLUSIONS

ASIAS is successful instrument that determines the attitude of a satellite by performing man algorithms on images of stars acquired by its onboard camera. The main advantage of ASIAS is its small size and extremely low cost. The ASIAS team was able to fully assemble a physical structure through the integration of complex hardware and software components within the budget of C\$1000. This renders ASIAS as the best candidate for primary attitude sensor for low-budget missions, such as nanosatellites and microsatellites. In retrospect, a great deal of experience was gained throughout the development of this project. The ASIAS team is grateful for the skills and knowledge they have gained during the design, construction and integration phases. Like any project, the ASIAS team has many things they would like to do to improve the current design, however the project is considered to be a successful accomplishment overall. All of the ASIAS hardware and software has been donated to Quine with the hope that future work

will be done to ensure that ASIAS will one day be a viable space component for satellites.

14 REFERENCES

- [1] – Hancock, B.R. et. al. “CMOS Active Pixel Sensor Specific Performance Effects on Star Tracker / Imager Position Accuracy”. California Institute of Technology, 2002
- [2] - Liebe, C.C. “Accuracy Performance of Star Trackers – A Tutorial”. California Institute of Technology, 2002
- [3] - Quine, B. “Spacecraft Guidance Systems – Attitude Determination using Star Camera Data”. University of Oxford, 1996.
- [4] - Samaan, M. “Towards Faster and More Accurate Star Sensors Using Recursive Centroiding and Star Identification”. Texas A&M, 2003.
- [5] - Wertz, J.R, Larson, W.J. “Space Mission Analysis and Design”. Microcosm Press, 1999.
- [6] - Dever, J.A, et al. “Indium Tin Oxide-Magnesium Fluoride Co-Deposited Films for Spacecraft Applications”. International Conference on Metallurgical Coatings and Thin Films, 1996.
- [7] - Sramek, N. “Radiation Hardened Electronics for Space Subsystems”. The Aerospace Corporation, 2001.
- [8] - Hiemstra, D. Keynote Address. ENG3330 Space Engineering Materials Class Lecture. York University, Feb. 2005.
- [9] - Kawano, H, et al. “New Light Shielding Technique for Shortening the Baffle Length of a Star Sensor”. SPIE - The International Society for Optical Engineering, 2002.
- [10] - www.matweb.com “Matweb – Materials Data Sheet”. Accessed Feb. 2007.
- [11] - “Soyuz User’s Manual”. Starsem, 2001.

APPENDIX A – Source Code for Algorithms

A.1 Centroiding Function (centroiding.m)

```
%%%%%-----  
%%% Centroiding Function: Supports Star_comparison.m  
%%% Author: Scott Mulligan  
%%% Note: +Xc right, -Xc left, +Yc down, -Yc up  
%%%-----  
  
function [Xc,Yc] = centroiding(r,c,I)  
  
num1=0;  
num2=0;  
den=0;  
xi=0;  
yi=0;  
  
for i=r-1:r+1;  
    xi=xi+1;  
    yi=0;  
    for j=c-1:c+1;  
        yi=yi+1;  
        num1 = int16(num1) + int16(xi) * int16(I(i,j));  
        num2 = int16(num2) + int16(yi) * int16(I(i,j));  
        den = den + int16(I(i,j));  
    end  
end  
  
Yc = (double(num1)/double(den))-2;  
Xc = (double(num2)/double(den))-2;
```

A.2 Data Analysis Algorithm (star_comparison.m)

```
%%%%%-----  
%%% Data Analysis Algorithm  
%%% Author: Scott Mulligan  
%%%-----  
  
clear all;  
  
flag = 0;  
Image_Number=0;  
  
while (flag == 0)  
    Image_Number = Image_Number + 1;  
  
    %% Set # of pixels, pixel size, 1st sigma, focal length, time interval  
    rows = 48;  
    columns = 86;
```

```

a = 7.5e-6;
b = 7.5e-6;
sigma=1.7453e-5;
f=0.05/a;
deltaT=1;

%%%% Read in image. Image name changed autonomously
%string1 = 'startest';
%string2 = int2str(Image_Number);
%Current_Image = strcat(string1, string2);
%I = imread(Current_Image,'bmp');
%imagerescale(I);

%%%% Read in intensity array from LabView
I = dlmread('pic.log')
imagerescale(I,[0 255]); colormap(gray);

Xc=0;
Yc=0;
D=0;
row_array=0;
column_array=0;
Xcoord=0;
Ycoord=0;
Xplane=0;
Yplane=0;
wD=0;
cart=0;
Star2Int=0;
Star3Int=0;
centerVal=0;
TargetStar=0;
star2=0;
star3=0;
count=0;

%%%% -----
%%%% Begin iteration through each pixel in search for stars
%%%% -----
for r = 6:rows-7;
    for c = 6:columns-7;

        if (((I(r,c)>95)&&(I(r-1,c-1)>35)&&(I(r-1,c)>35)...
            &&(I(r-1,c+1)>35)&&(I(r,c-1)>35)&&(I(r,c+1)>35)...
            &&(I(r+1,c-1)>35)&&(I(r+1,c)>35)&&(I(r+1,c+1)>35)...
            &&I(r,c)>I(r-1,c-1))&&(I(r,c)>I(r-1,c))&&(I(r,c)>I(r-1,c+1))...
            &&(I(r,c)>I(r,c-1))&&(I(r,c)>I(r,c+1))&&(I(r,c)>I(r+1,c-1))...
            &&(I(r,c)>I(r+1,c))&&(I(r,c)>I(r+1,c+1)))

        %% Count # of stars identified, and record their pixel location
        count=count+1;
        row_array(count) = r;
        column_array(count) = c;

        %% Call cenroiding function
        [Xc(count),Yc(count)]=cenroiding(r,c,I);
    end
end

```

```

%%%% Calculate star coordinates in the image plane
Xcoord(count) = c+Xc(count);
Ycoord(count) = r+Yc(count);
Xplane(count) = ((Xcoord(count)-(rows/2))/f);
Yplane(count) = ((Ycoord(count)-(columns/2))/f);

%%%% Calculate total intensity of star from 9 pixels
StarIntensity(count) = int16(I(r-1,c-1))+int16(I(r-1,c))+int16(I(r-1,c+1))...
+int16(I(r,c-1))+int16(I(r,c+1))+int16(I(r+1,c-1))+int16(I(r+1,c))+int16(I(r+1,c+1));

%%%% Convert Image plane coordinates to Cartesian coords
part1=(1/(sqrt(Xplane(count)^2+Yplane(count)^2+1)));
cart(1,count) = part1*(-Xplane(count));
cart(2,count) = part1*1;
cart(3,count) = part1*(-Yplane(count));

for iterate = count-1:-1:1;
    wD(count,iterate) =
    acos((cart(1,count)*cart(1,iterate))+(cart(2,count)*cart(2,iterate))+(cart(3,count)*cart(3,iterate)));
    wD(iterate,count) = wD(count,iterate);
end
end
end

%%%% -----
%%%% Construct Star Triad
%%%% -----
run=0;
while (star2==0 && star3==0)

%%%% Find Target Star in Image
if (run>0)
    centerVal(ind)=10000;
    for i=1:(length(centerVal)-1)
        centerVal(i)=centerVal(i+1);
    end
    if (run==length(centerVal))
        break
    end

elseif (run==0)
    for i=1:count;
        centerVal(i) = sqrt((Xcoord(i)-(columns/2))^2+(Ycoord(i)-(rows/2))^2);
    end
end
[val,ind]=min(centerVal);
TargetStar = ind;

%%%% Find the 2nd and 3rd star to create Triad
for i=1:count;
    if (StarIntensity(i)>Star2Int && wD(TargetStar,i)<0.004 && wD(TargetStar,i)>0.000117)
        Star2Int = StarIntensity(i);
        star3 = star2;
        star2 = i;
    end
end

```

```

elseif (StarIntensity(i)>Star3Int && wD(TargetStar,i)<0.004 && wD(TargetStar,i)>0.000117)
    Star3Int = StarIntensity(i);
    star3 = i;
end
end

run = run+1;
end

%%%%%
%%%%% Mark star locations chosen
%%%%%
hold on;

%%%%% Mark all stars
plot(Xcoord,Ycoord,'ro')
plot(column_array,row_array,'bx')
plot(Xcoord(TargetStar),Ycoord(TargetStar),'ro','MarkerSize',10,'LineWidth',3)

if (star2~=0 && star3~=0)

    plot(Xcoord(star3),Ycoord(star3),'bo','MarkerSize',10,'LineWidth',3)
    plot(Xcoord(star2),Ycoord(star2),'bo','MarkerSize',10,'LineWidth',3)
    line1 = [Xcoord(TargetStar),Xcoord(star2)];
    line2 = [Ycoord(TargetStar),Ycoord(star2)];
    line3 = [Xcoord(TargetStar),Xcoord(star3)];
    line4 = [Ycoord(TargetStar),Ycoord(star3)];
    line5 = [Xcoord(star2),Xcoord(star3)];
    line6 = [Ycoord(star2),Ycoord(star3)];
    plot(line1,line2,'y','LineWidth',4)
    plot(line3,line4,'y','LineWidth',4)
    plot(line5,line6,'y','LineWidth',4)

S1 = TargetStar
S2 = star2
S3 = star3

triad = [S1 S2 S3]
dlmwrite('Triad.txt', triad, ',')

dist1 = wD(S1,S2)
dist2 = wD(S1,S3)
dist3 = wD(S2,S3)

triad_dist = [dist1 dist2 dist3]
dlmwrite('Triad_Dist.txt', triad_dist, ',')
end

%%%%%
if (Image_Number>1)
    bi2 = bi;
    %bi_cross2 = bi_cross;
end

%%%%%

```

```

if (Image_Number == 1)
    flag = 1;
end

end

```

A.3 Average Distance to Center of Image Plane (PixelDist.m)

```

%%%% Title: Average Pixel Distance
%%%% Author: Scott Mulligan
%%%% Calculates the average distance from star ...
%%%% to center of the image plane

```

```

runs = 1000000000;
Xpixels = 648;
Ypixels = 488;
totalDist = 0;

for i = 1:runs;

    X = (rand-0.5)*Xpixels;
    Y = (rand-0.5)*Ypixels;
    totalDist = totalDist+((X^2+Y^2)^0.5);

end

Avg_Distance = totalDist/runs

```

A.4 Field of View Simulation Algorithm (FoV_sim.m)

```

%%%%-----
%%%% Celestial Sphere with star coordinates
%%%% Author: Scott Mulligan
%%%% Helps determine proper FoV for ASIAS
%%%%-----

```

```

clear all;
FoV_size = 5
FoV = FoV_size*pi/180;
Magnitude_trunc = 7.65;

%%%% Read in star catalogue (Hipparcos data)
fid = fopen('finaldata.txt');
C = textscan(fid, '%f %f %f %f %f');
fclose(fid);

%%%% Convert data from file to radians
C{2}=C{2}*pi/180;
C{3}=C{3}*pi/180;
C{4}=C{4}*pi/180;

```

```

C{5}=C{5}*pi/180;

radius=1;

%%%% Truncate stars above certain V magnitude
n=0;
for i = 1:118209;
    if ((C{6}(i))<Magnitude_trunc)
        n=n+1;
        array1(n)=C{1}(i);
    end
end

array2(n)=0;
array3(n)=0;
array4(n)=0;
array5(n)=0;
array6(n)=0;

k=0;
for i = 1:118209;
    if ((C{6}(i))<Magnitude_trunc)
        k=k+1;
        array2(k)=C{2}(i);
        array3(k)=C{3}(i);
        array4(k)=C{4}(i);
        array5(k)=C{5}(i);
        array6(k)=C{6}(i);
    end
end

Mag_Limit = n

%[x,y,z] = sph2cart(array2,array3,radius);
%plot3(x,y,z,'x');
%figure;

[array2X,array2Y,array2Z] = sph2cart(array2,array3,1);

insphere=0;
R=2;
%%%%-----
%%%% Iterate FoV calculations to create histogram
%%%%-----
for j = 1:20000;

%%%% Randomly generate celestial coordinates in unit box
randX = (rand-0.5)*2;
randY = (rand-0.5)*2;
randZ = (rand-0.5)*2;
%%%% Convert random coordinates to RA & Dec
[THETA,PHI,R] = cart2sph(randX,randY,randZ);

if ((R<=1)&&(insphere<10000))

```

```

insphere=insphere+1;

[finalX,finalY,finalZ] = sph2cart(THETA,PHI,1);

k=0;
for i = 1:n;

    if (acos(finalX*array2X(i) + finalY*array2Y(i) + finalZ*array2Z(i)) < FoV/2)
        k=k+1;
    end
end

Stars_in_FoV(insphere) = k;

end

if (insphere>=10000)
    break;
end

end

%%%% Plot Histogram
x=0:50;
hist(Stars_in_FoV,x)
title('Histogram: Number of Stars in FoV','FontSize',14)
xlabel('Number of Stars Visible in FoV','FontSize',12)
ylabel('Frequency','FontSize',12)
axis tight;

%%%% Calculate what % of trials have more than 3 stars
Percent_more_than=0;
for i = 1:length(Stars_in_FoV);
    if (Stars_in_FoV(i)>=5)
        Percent_more_than = Percent_more_than+1;
    end
end
Atleast_5 = Percent_more_than/length(Stars_in_FoV)

Percent_more_than2=0;
for i = 1:length(Stars_in_FoV);
    if (Stars_in_FoV(i)>=1)
        Percent_more_than2 = Percent_more_than2+1;
    end
end
Atleast_1 = Percent_more_than2/length(Stars_in_FoV)

avg = sum(Stars_in_FoV/insphere)

```

APPENDIX B – Space Qualification Testing

B.1 Vibration Test Procedure

Date: 24 April 2007

Time: 10:30-11:30AM

Project Team: Autonomous Star Imaging Attitude Sensor (ASIAS)
Qualification Test: Vibrational Loading Test

Location: CRESS Laboratory, Petrie Science and Engineering Building, York University

Duration: 1 hour @ C\$65/hour

Laboratory Technician: Rajinder Jagpal

Team Representative: Matthew Cannata

Description:

Part of the preliminary space-qualification tests for the ASIAS star-tracker component. The point of the test is to see how the hardware reacts to launch loads, and how the testing affects the functionality of the system. Tests have been designed using the typical maximum values of loading when launching on the Soyuz system, without any safety factors being included.

Testing Conditions:

The testing will take place in local laboratory environmental conditions, which are assumed to be around Standard Ambient Temperature and Pressure (SATP).

The component will be secured to the vibrational loader using the same mounting bracket and fastening method that was used for Dr. B. Quine's ARGUS component (consult that project for more information). Both ASIAS and the vibrational loader will be monitored using the laboratory's accelerometers.

ASIAS will be disconnected and in its powered-off mode for the duration of the test.

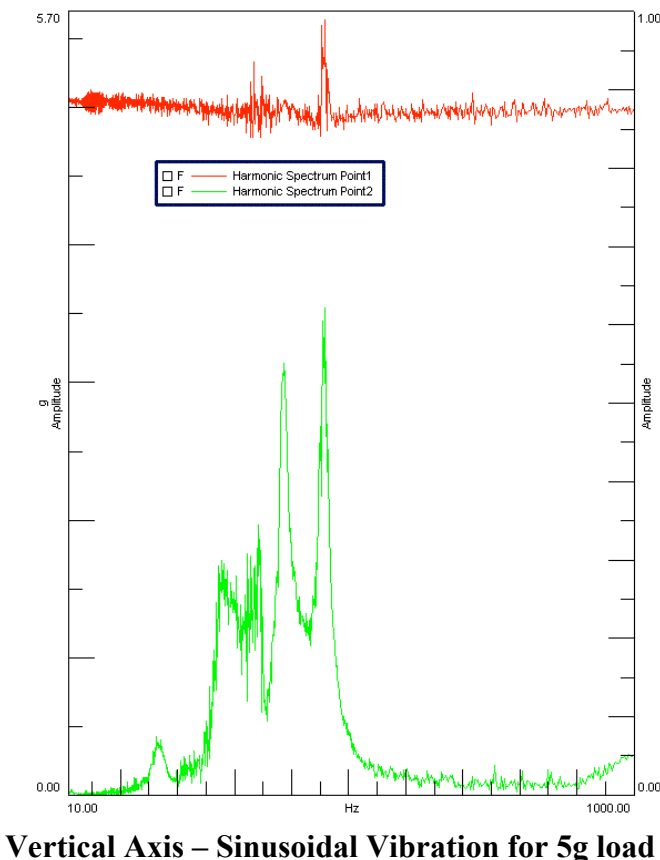
Testing Procedure:

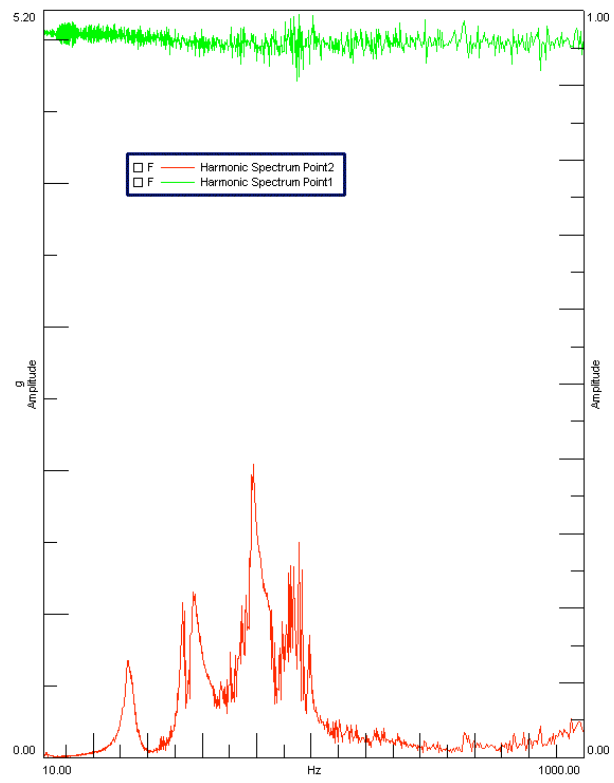
1. Calibrate ASIAS.
2. Mount ASIAS to the loader with the baffle facing upwards.
3. Using the parameters on the following table, complete the tests one after the other.

4. Mount ASIAS to the loader with its lid facing away from the mounting bracket.
5. Repeat Step 3.
6. Determine the functionality of ASIAS, including calibration errors introduced in the testing.

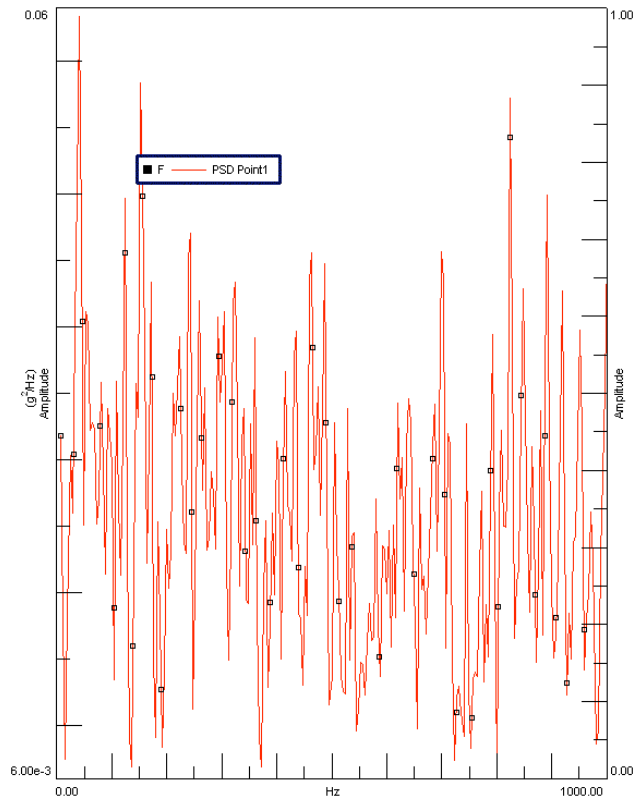
NOTE: All vibrations are occurring at 4g's, the maximum longitudinal loading of the rocket during launch. This has been factored into the test amplitudes.					
Test Number	Description of Vibrations	Duration (s)	Frequency (Hz)	Amplitude (g – Force of gravity)	Spectral Density ($10^{-3} \text{ g}^2/\text{Hz}$)
1	Sine-equivalent	180	10 to 1000 to 10	5.0	
2	Random	120	10 to 1000		5.0 (RMS)

B.2 Vibration Test Results





Longitudinal Axis – Sinusoidal Vibration for 5g load:



Vertical Axis – Random Vibration for 5g load

B.3 Vacuum Test Procedure

Date: 26 April 2007

Time: 09:30-11:30

Project Team: Autonomous Star Imaging Attitude Sensor (ASIAS)
Qualification Test: Thermal Vacuum Test

Location: CRESS Laboratory, Petrie Science and Engineering Building, York University

Duration: 2 hours (charged 1 hour @ C\$65/hour)

Laboratory Technician: Rajinder Jagpal

Team Representative: Vlad Popovici

Description:

Part of the preliminary space-qualification tests for the ASIAS star-tracker component. The point of the test is to see how the hardware reacts to the space environment, and how the testing affects the functionality of the system. It is assumed that ASIAS is an internal component in a spacecraft bus. This bus is responsible for radiation properties, and as such ASIAS will only be tested in a vacuum environment and not a thermal environment.

Testing Conditions:

The testing will take place in local laboratory environmental conditions, which are assumed to be around Standard Ambient Temperature and Pressure (SATP).

The component will be sitting in the chamber, along with a component from another team. The two components will not interact.

ASIAS will be connected and in its powered-on mode for the duration of the test. Data will be streamed outside the chamber via the chamber's 9-pin RS232 port, with the appropriate connections being interfaced (see attached page for pin-out diagram).

Testing Procedure:

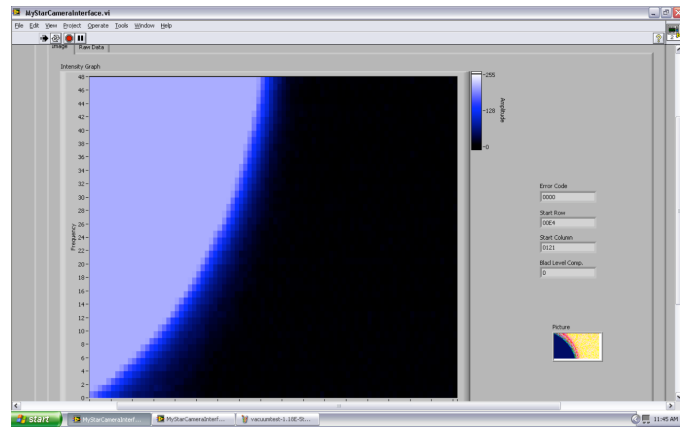
7. Calibrate ASIAS.
8. Place ASIAS in the chamber, and connect to the chamber's port.
9. Establish the functionality of ASIAS in the chamber.
10. Lower the pressure in the chamber to 10^{-6} torr for 2 hours. Every 15 minutes, determine the functionality of ASIAS.
11. Raise the pressure of the chamber, and remove ASIAS.

12. Determine the functionality of ASIAS, including errors introduced in the testing.

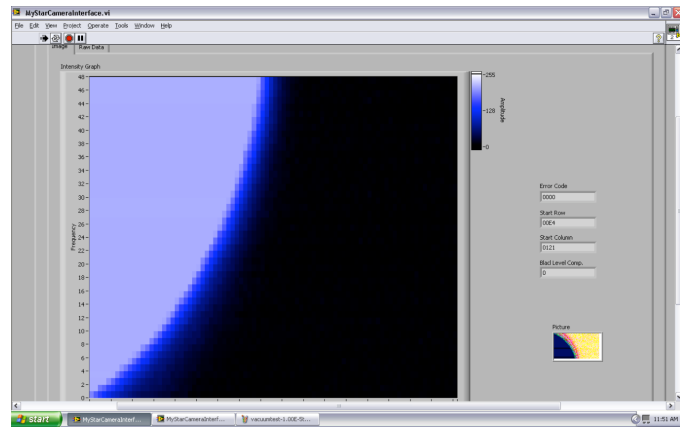
B.4 Vacuum Test Results

The following results demonstrate that ASIAS was fully functional and remained calibrated during the vacuum test.

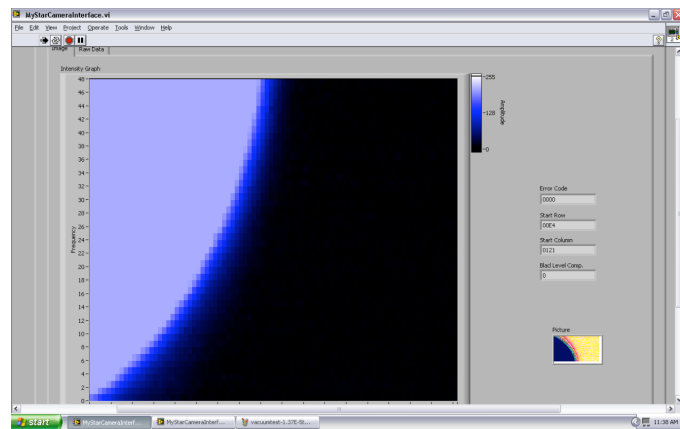
Picture of the LED at 10^{-2} torr:

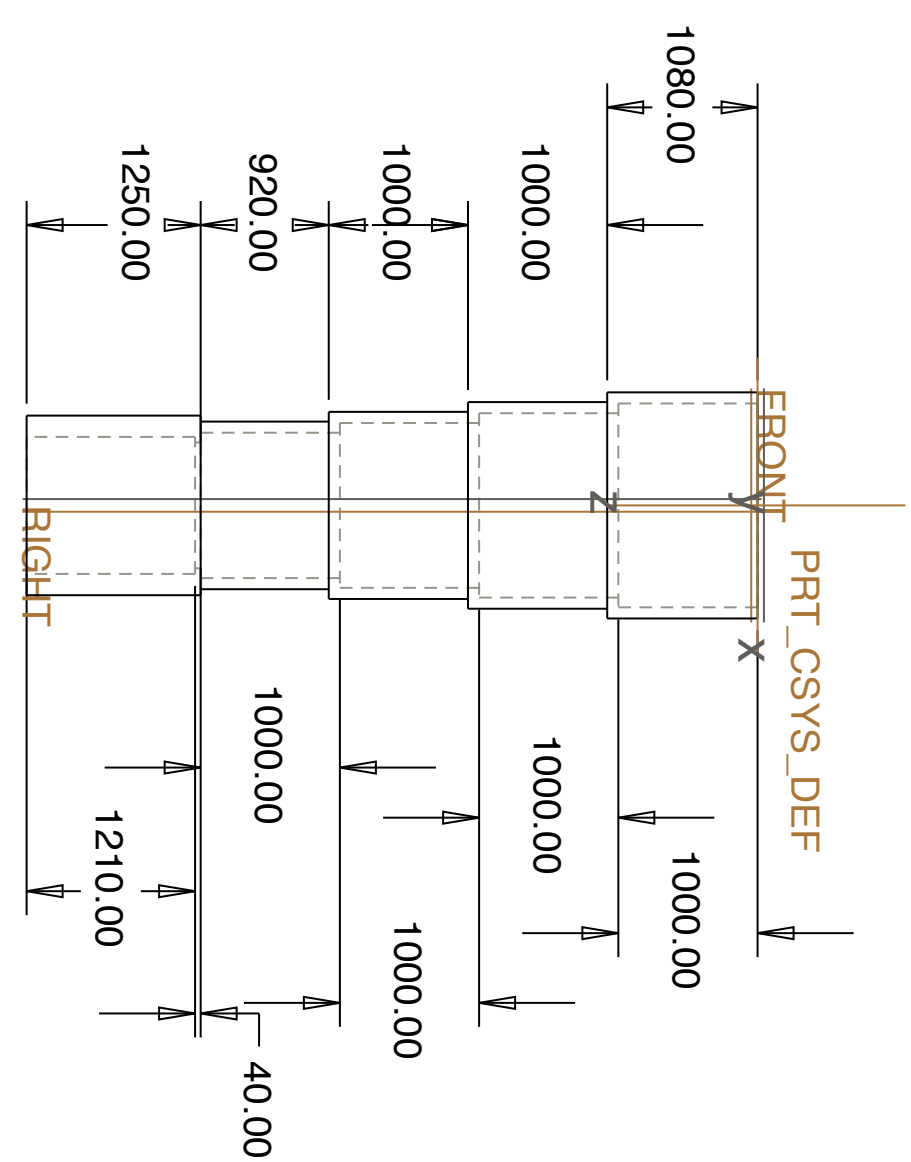


Picture of the LED at 10^{-4} torr:

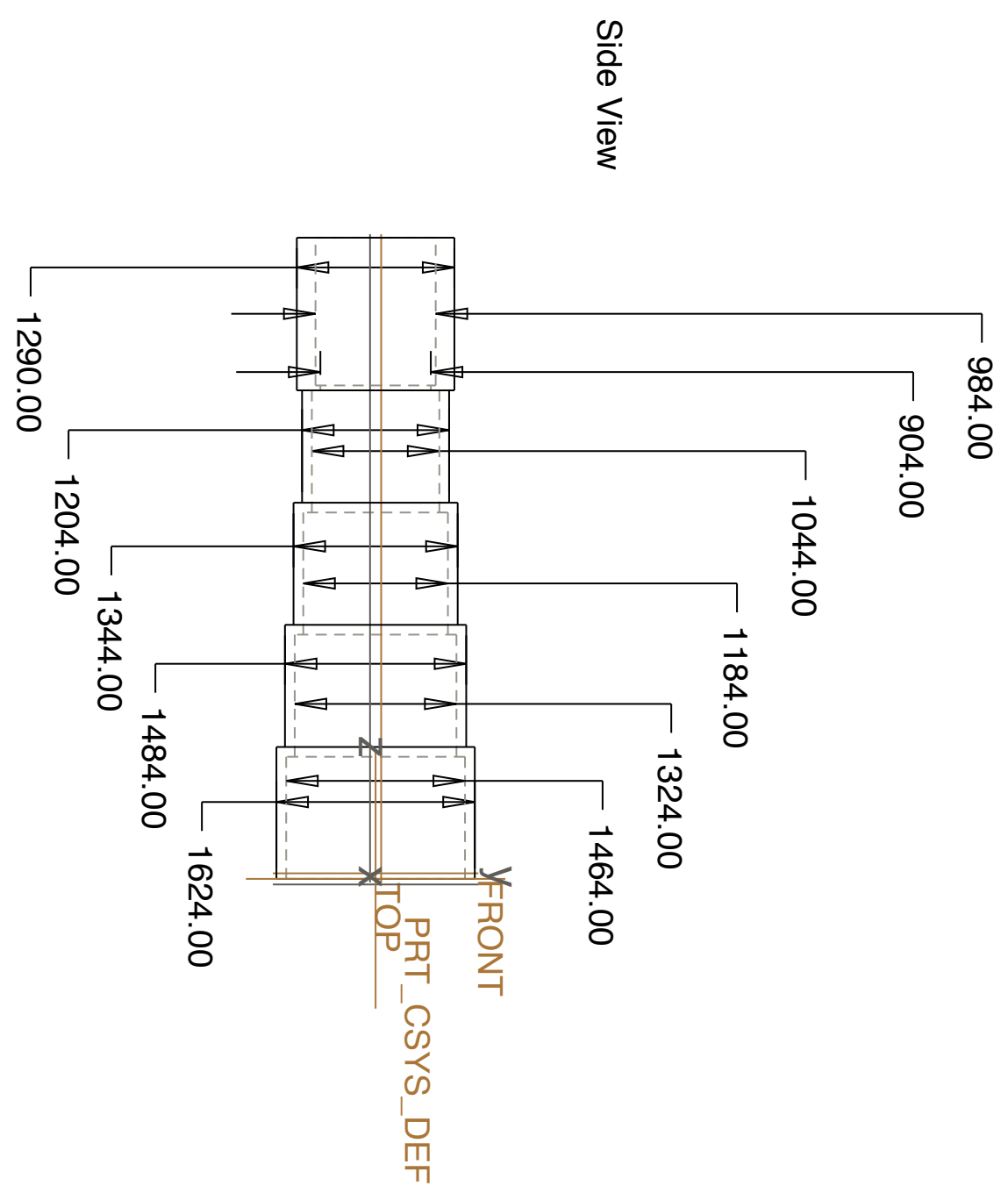


Picture of the LED at 10^{-6} torr:





BAFFLE - ALL DIMENSIONS IN THOUSANDTHS OF AN INCH (mil)



Top View

APPENDIX C

69.00

R56.00

3250.00

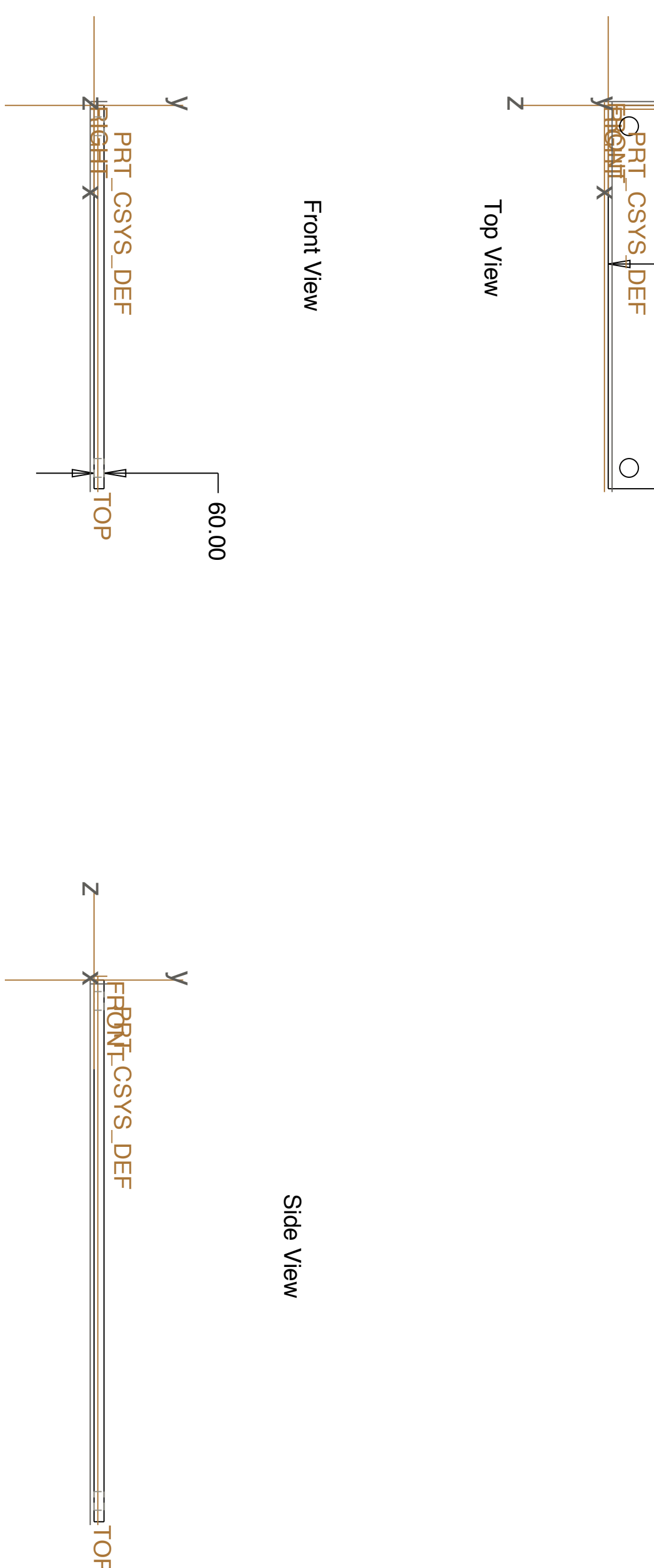
2300.00

Front View

Side View

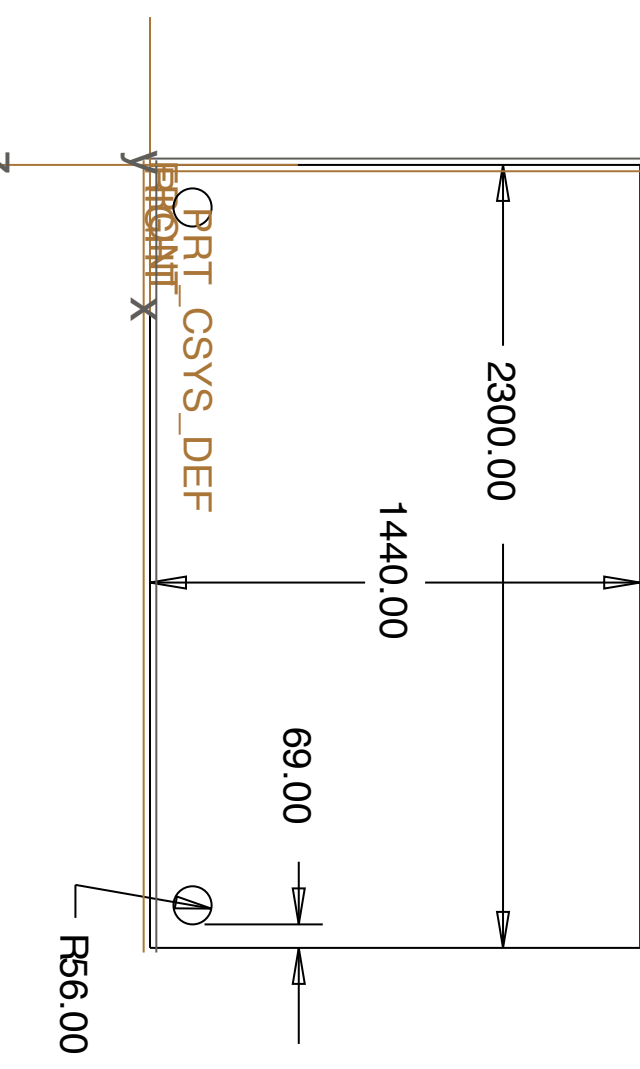
APPENDIX D, PART 1

MICROCONTROLLER AND DAUGHTER BOARD - ALL DIMENSIONS IN THOUSANDS OF AN INCH (mil)



APPENDIX D, PART 2

SENSOR BOARD - ALL DIMENSIONS IN THOUSANDTHS OF AN INCH (mil)



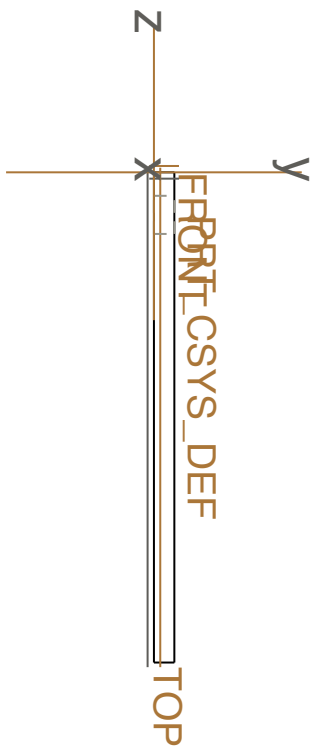
Front View (Upside Down)

The optical centre of the CMOS sensor is 600mils from the right and 640mils

from the bottom edges, rightside up

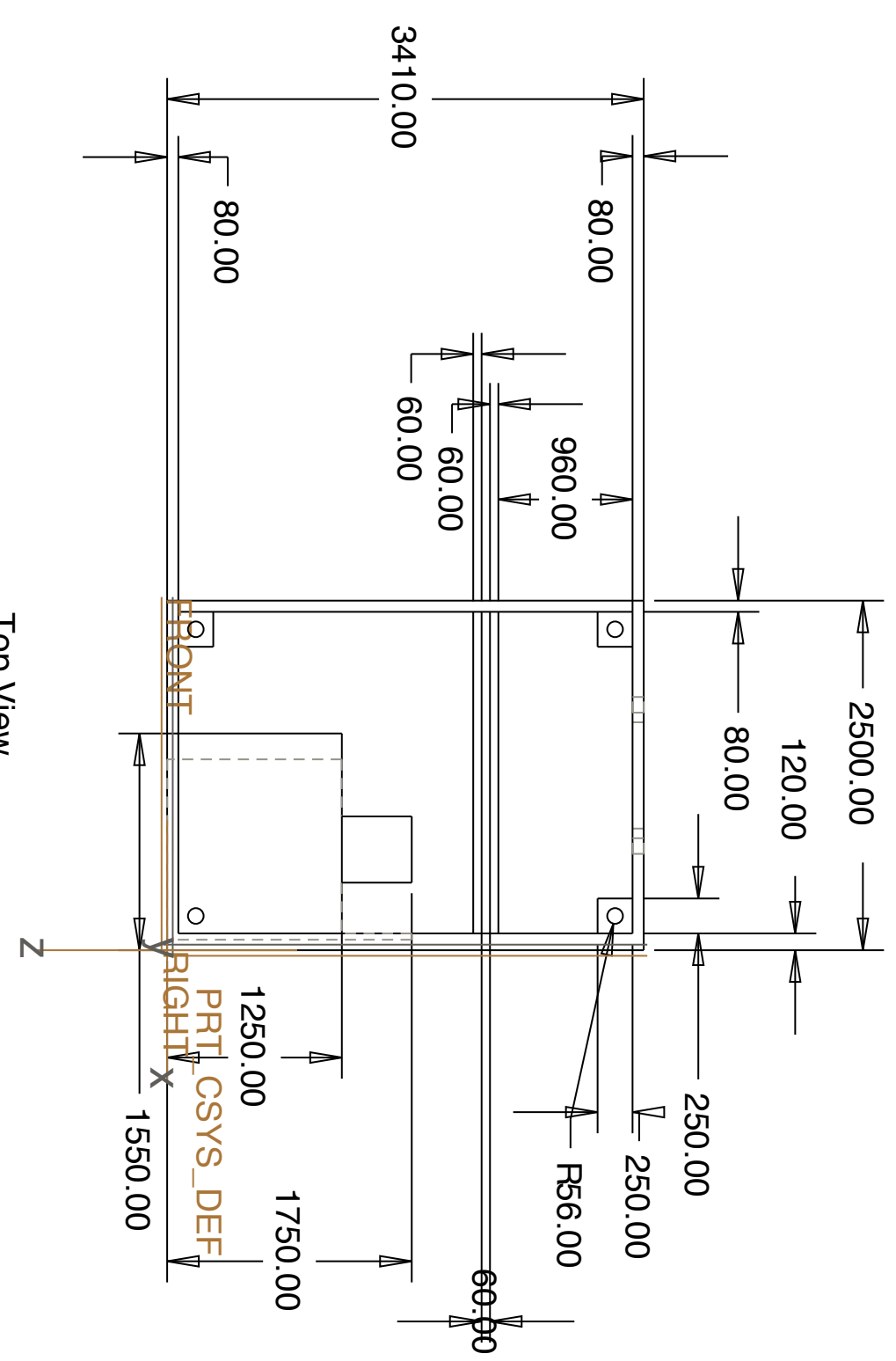


Top View



Side View

APPENDIX E

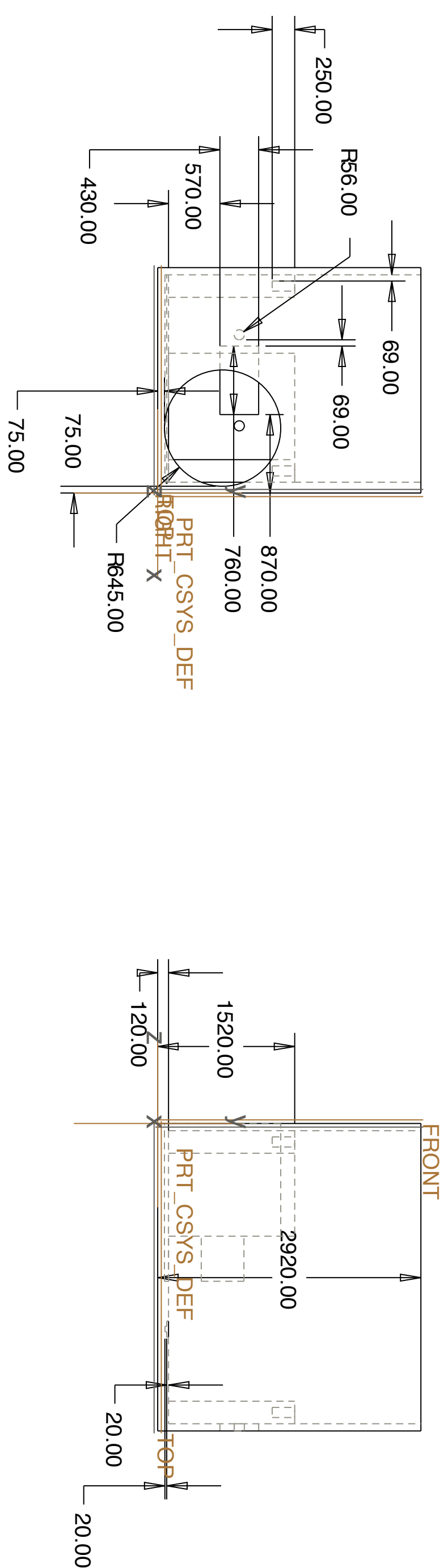


STRUCTURE - ALL DIMENSIONS IN THOUSANDTHS OF AN INCH (mil)

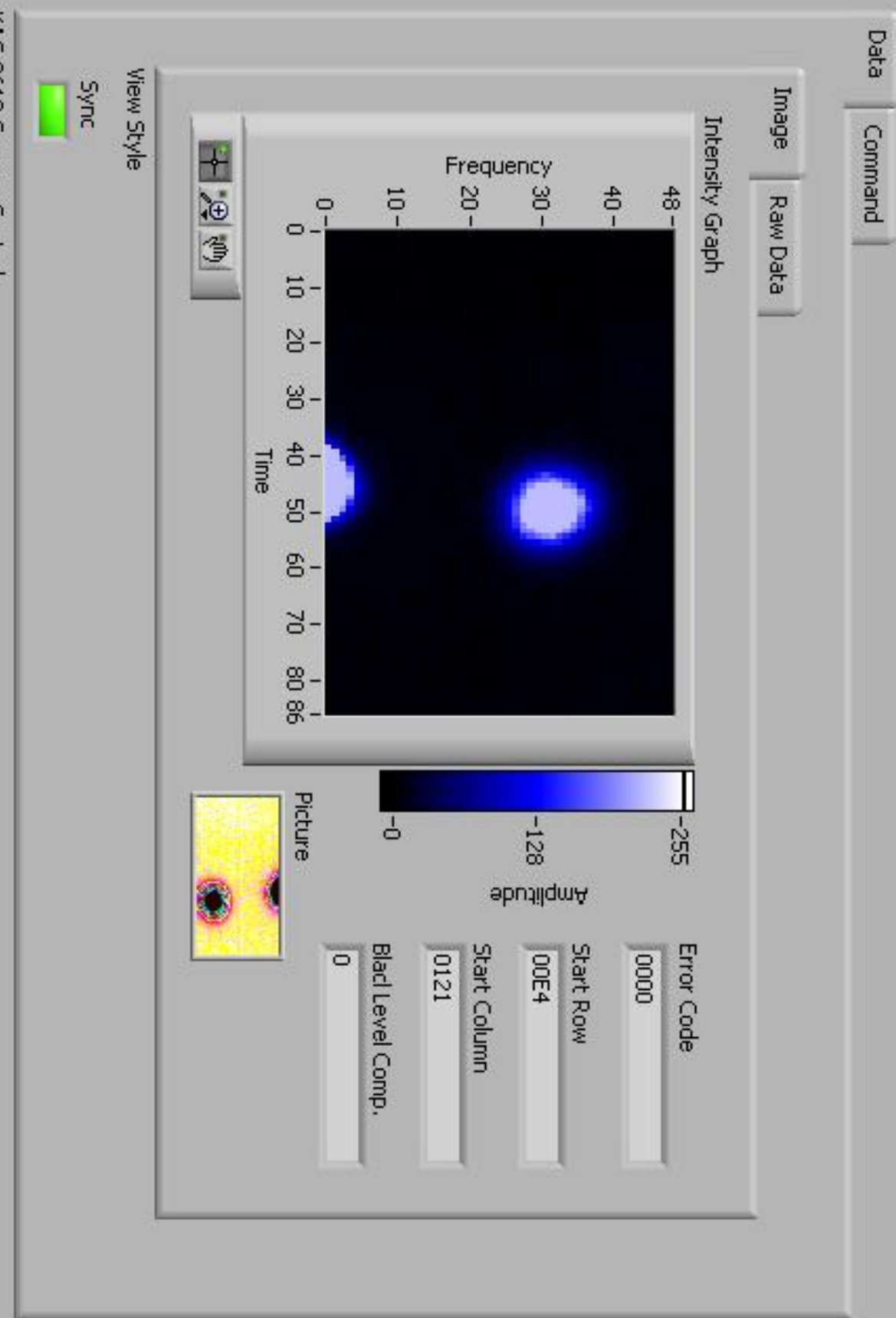
Front View

Baffle hole is threaded with 15mil deep threads, 32 per inch

Right View



Appendix F, Part 1
– LabView Front Panel



Appendix F, Part 2 – Portion of LabView Block Diagram

